MATERIAL PARAMETERS AND CREEP IN A ROTATING COMPOSITE CYLINDER

A Thesis report submitted
in partial fulfilment of the requirements for
the award of degree of

MASTER OF ENGINEERING
IN
CAD/CAM & ROBOTICS

Submitted by

KAPIL SACHAN

ROLL NO.8048111

Under the Guidance of

Dr.V.K.GUPTA
Reader, M.E.D.
Univ.College of Engineering
Punjabi University,Patiala

Mr. TARUN NANDA
Lecturer, M.E.D.
T.I.E.T, Patiala

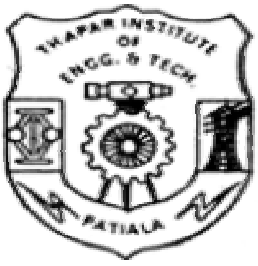

MECHANICAL ENGINEERING DEPARTMENT
THAPAR INSTITUTE OF ENGINEERING AND TECHNOLOGY
(DEEMED UNIVERSITY) PATIALA-147004, PUNJAB

MAY, 2006

No human investigation can claim to be scientific
if it doesn't pass the test of mathematical proof.

- ALBERT EINSTEIN

Do all the good you can,
By all the means you can,
In all the ways you can,
In all the places you can,
At all the times you can,
To all the people you can,
As long as ever you can.

- JOHN WESLEY

CERTIFICATE

This is to certify that the thesis titled, **"MATERIAL PARAMETERS AND CREEP IN A ROTATING COMPOSITE CYLINDER**", being submitted by **Mr. KAPIL SACHAN,** in partial fulfillment of the requirement for the award of degree of **MASTER OF ENGINEERING (CAD/CAM & ROBOTICS)** at **Mechanical Engineering Department**, **Thapar Institute of Engineering and Technology (Deemed University), Patiala,** is a bonafide work carried out by him under our guidance and supervision and that no part of this seminar has been submitted for the award of any other degree.

Dr. V. K. GUPTA
Reader,
Deptt. of Mechanical Engineering,
Univ. College of Engg.,
Punjabi University, Patiala-147002.

Mr. TARUN NANDA
Lecturer,
Deptt. of Mechanical Engineering,
T. I. E. T, Patiala-147004.

(Dr. S.K. Mohapatra)
Professor& Head, M.E.D.,
Thapar Inst.of Engg. &Tech.
Patiala-147004 (Punjab)

(Dr. T.P.Singh)
Dean Academic Affairs
Thapar Inst. of Engg. & Tech.
Patiala-147004 (Punjab)

ACKNOWLEDGEMENT

I express my sincere gratitude to my guides, **Dr V.K.Gupta**, Reader, **Mechanical Engineering Department, Univ.College of Engg, Punjabi University** and **Mr. Tarun Nanda,** Lecturer, **Mechanical Engineering Department, Thapar Institute of Engineering & Technology,** for their valuable guidance, proper advice and constant encouragement during the course of my work on this thesis. Without their help this report wouldn't have seen the light of the day.

I am also grateful to our PG-Coordinator **Dr. Vijay Kumar Jadon** for successfully carrying the framework for the thesis.

I am also thankful to all my friends, who devoted their valuable time and helped me in all possible ways towards successful completion of my thesis work

I do not find enough words with which I can express my feeling of thanks to entire faculty and staff of **Mechanical Engineering Department, Thapar Institute of Engineering & Technology,** for their help, inspiration and moral support, which went a long way in successful completion of my thesis.

(KAPIL SACHAN)

Roll No. 8048111

ABSTRACT

The steady state creep in a rotating cylinder made of isotropic aluminium-silicon carbide particulate composite has been investigated in the present study. The creep behaviour of the composite has been described by Sherby's law. The creep parameters in the law have been extracted from the available experimental results for Al-SiC_P under uniaxial creep. The radial, tangential and axial stresses and steady state creep rates in the cylinder have been calculated and presented for various combinations of material parameters (like particle size and particle content) and temperatures. The study revealed that the stress distributions in the cylinder do not vary significantly for various combinations of particle size, particle content and operating temperature except for slight variation observed for varying particle content. However, the tangential as well as radial strain rates in the cylinder decrease significantly with decreasing SiC_p size, with increasing SiC_p content and with decreasing operating temperature.

INDEX

CONTENTS Page No.

LIST OF FIGURES

Figures **Page No.**

CHAPTER 1

INTRODUCTION

The continuing quest for improved performance, specified in terms of weight reduction, high strength and low cost has led to develop a new class of materials called composite materials.

A composite material consists of combining two or more constituents called matrix and reinforcement. The constituents are combined at microscopic level and are not soluble to each other. Matrix phase materials are generally continuous while the reinforcing phase may be in the form of fibers, particles or flakes.

The composite materials possess characteristic properties, such as high stiffness, high strength, low weight, high temperature performance, good corrosion resistance, high hardness and conductivity that are not possible in any of its constituents alone. Analysis of these properties reveals that they depend on the following:

a) Properties of the individual constituents.
b) Relative amounts of the constituents.
c) Size and shape of the constituents (i.e. Morphology).
d) Degree of bonding between constituents.
e) Orientation of the various constituents.

The composite materials possess high specific modulus and specific strength as compared to conventional materials. Specific Modulus is defined as the ratio of Young Modulus and density whereas Specific Strength is defined as the ratio of strength and density of materials. As an example the strength of a graphite/epoxy unidirectional composite material is same as that of steel but specific strength of this composite is three times that of steel thereby saving in cost of material and energy [1].

1.1 Parameters for Selection of Composites

For selecting a composite material for a particular application, the following parameters are to be considered:

(i) Strength

(ii) Toughness

(iii) Formadibility

(iv) Weldeability

(v) Corrosion

(vi) Wear Resistance

(vii) Affordability.

1.2 Factors affecting Mechanical Performance

The mechanical performance of composite materials depends on number of factors such as:

I) Fiber factor

II) Matrix factor

III) Other factors (Fiber Matrix interface, etc.)

I) Fiber factor:

It involves the following four parameters.

a) Length

b) Orientation

c) Shape

d) Material

a) Length: - Fiber can be either short or long in the length as shown in Fig.1.1.

(a) **(b)**

Fig.1.1 (a) Short fiber Composite (b) Long fiber Composite [1].

Long continuous fibers are easy to orient and process while short fibers cannot be fully controlled or oriented properly. Further, long fibers provide several benefits over short fibers including high impact resistance, low shrinkage, improved surface finish and dimensional stability. On the other hand, short fibers provide low cost, easy to work with and have fast cycle time fabrication procedures. Short fibers possess few flaws, therefore leading to higher strength.

b) Orientation: - The distribution of fiber in a matrix can be random or aligned in a specific direction to achieve very high stiffness and strength in that direction. If fibers are oriented in more than one direction in matrix, the composite will exhibit possess high stiffness and strength along these directions.

c) Shape: - The most common shape of fibers is circular because of ease of handling and manufacturing. Hexagonal and square-shaped fibers are possible but their advantages of strength and high packing factors do not out weigh the difficulty in handling and processing.

d) Material: - The material of fiber directly influences the mechanical performance of a composite. Fibers are generally expected to have high elastic modulus and strength. This expectation along with the low cost are the key factors that graphite, aramids and glass fibers dominate the fiber market for composites.

II) Matrix Factors

Fibers are used as reinforcement to matrix. The matrix functions include binding of the fibers together, protecting fibers from environment, shielding from damage during handling and load transfer from matrix to fibers. In general, the matrix possesses inferior properties compared fibers.

III) Other Factors

Apart from fiber and matrix there are several other factors which can affect the mechanical performance of composite materials. The fiber-matrix interface is an important factor which determines how well the matrix transfers the loads to the fibers. The fiber-matrix interfacial bonding is of following three types:

a) Chemical Bonding
b) Mechanical Bonding
c) Reaction Bonding

a) Chemical Bonding

Chemical bonding is formed between the fiber surface and the matrix. Some fibers bond naturally to the matrix while others do not. Coupling agents are often added to form a chemical bond.

b) Mechanical Bonding

Natural roughness and etching of the fiber surface causing interlocking may form a mechanical bond between the fiber and the matrix. If the coefficient of thermal expansion of the matrix is higher than that of fiber, and the manufacturing temperatures are higher than the operating temperatures, the matrix will shrink more than the fiber, causing the compression of matrix around the fiber.

c) Reaction Bonding

Reaction bonding occurs when atom or molecules of fiber and matrix diffuse into each other at interface. This inter diffusion often creates a distinct interfacial layer, which has different properties than that of fiber or matrix. Though, this thin layer helps to form a bond but it also forms micro cracks in the fiber. These micro-cracks reduce the strength of fiber which ultimately leads to poor strength of composite materials.

1.3 Classification of Composite Materials

Composites are classified [2] by the geometry of the reinforcement as particulate, flake and fiber or by the type of matrix as polymer, metal, ceramic and carbon as shown in Fig.1.2.

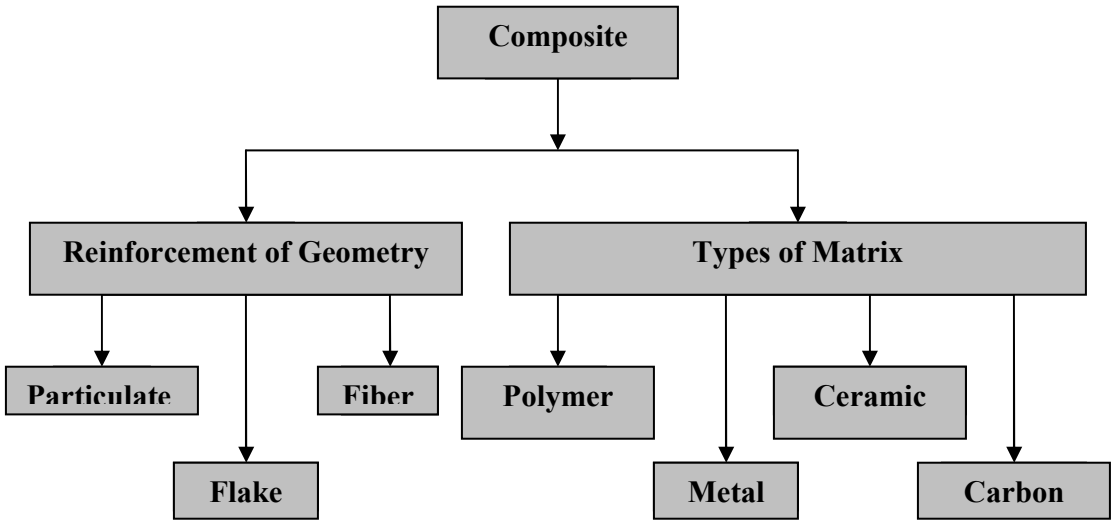

Fig 1.2: Classification of Composite materials

1.3.1 Classification based on Reinforcement Geometry

According to the reinforcement geometry, composites are classified into three groups, namely [1]:

a) Particulate Composites
b) Flake Composites
c) Fiber Composites

a) Particulate Composites

It consists of particles reinforced in matrices such as alloy and ceramics as shown in Fig.1.3 (a). They are usually isotropic since the particles are randomly distributed. Particulate composite has advantages such as improved strength, increased operating temperature and oxidation resistance etc. Examples include use of aluminum particles in rubber matrix, silicon particles in aluminum matrix etc.

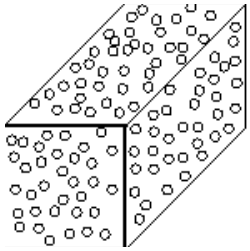

Fig.1.3 (a) Particulate Composite

(b) Flake Composites

It consists of flake shaped reinforcement such as glass, mica, silica, silver etc in matrices as shown in Fig.1.3 (b). Flake composites provide advantages such as high out of plane flexural modulus, higher strength and low cost. However, flakes can not be oriented easily therefore a limited number of materials are available for use.

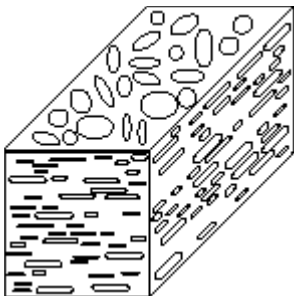

Fig.1.3 (b) Flake Composite

(c) Fiber Composites

It consists of matrix reinforced by short (discontinuous) or long (continuous) fibers as shown in Figs. 1.3(c). Fibers are generally anisotropic. Typical examples of matrices are resins such as epoxy, metals such as aluminum and ceramics such as calcium-alimino-silicate.

(i) **(ii)**

Fig.1.3 (c) (i) Short Fiber Composite (ii) Long Fiber Composite

1.3.2 Classification based on Matrix

Based on the type of matrix, Composites may be classified as [1]:

a) Polymer Matrix Composite (PMC)
b) Metal Matrix Composite (MMC)
c) Ceramic Matrix Composite (CMC)
d) Carbon–Carbon Composite

a) Polymer Matrix Composite (PMC)

These are the most common advanced composites consisting of polymer (epoxy, polyester, urethane etc) reinforced by thin diameter fibers (graphite, aramids, boron etc). Graphite/Epoxy composites are approximately five times stronger than steel on a weight-for-weight basis. They are commonly employed due to their low cost, high strength and simple manufacturing. Main drawbacks of polymer Laminate Composites (PMCs) include low operating temperature, high coefficient of thermal and moisture expansion and low elastic properties in certain directions. However, their advantages are high strength, low cost, high chemical resistance and good insulating property.

b) Metal Matrix Composite (MMC)

It consists of metal matrix such as aluminum, magnesium and titanium etc. reinforced with fibers such as carbon, silicon carbide etc. Metals are reinforced to increase or decrease their properties to suit the design needs. For example, the elastic stiffness and strength of metals can be increased, while large coefficients of thermal expansion and thermal and electric conductivities of metal can be reduced by addition of fibers such as silicon carbide.

MMCs are mainly used to provide advantages over monolithic alloy/metals such as steel and aluminum. These advantages include higher specific strength and specific modulus achieved by incorporation of reinforcement in low density metal matrix such as aluminum and titanium. MMCs possesses several advantages over polymer matrix composite such as higher elastic properties, higher service temperature, insensitive to moisture, higher electric and thermal conductivity, better fatigue and flow resistance. However, the drawbacks of MMCs over PMCs include higher processing temperature and higher densities.

c) Ceramic Matrix Composite (CMC)

Ceramic matrix composites (CMCs) have a ceramic matrix such as alumina, calcium-alumino-silicate reinforced by fibers such as carbon or silicon carbide. Their main advantages include high strength and hardness, high service temperature, chemical inertness and low density. CMCs are finding extensive applications in high temperature areas where MMCs and PMCs cannot be used.

d) Carbon–Carbon Composite

Carbon-carbon composites have carbon fiber reinforced in matrix of carbon. Carbon-carbon composites are used in very high temperature environments up to 6000 °F (3315°C) and are 20 times stronger and 30% lighter than graphite fibers. Their advantages include ability to withstand high temperatures, low creep at high temperature, low density, good tensile and compressive strength, high fatigue resistance, high thermal conductivity and high coefficient of friction. Their disadvantages include high cost, low shear strength and susceptibility to oxidations at high temperature. These composites find

application in space shuttle nose cone, aircraft brakes, mechanical fasteners etc.

1.4 Aluminium /Aluminium alloy based MMCs

MMCs based on aluminium and its alloys are widely used in engineering and structural applications due to their light weight, which is the primary requirement in most of the MMC's applications [2]. In addition to this, aluminium/aluminium alloy based MMCs are economical compared to other light metals, such as titanium and magnesium. The excellent strength, ductility and corrosion resistance of MMCs are well established and can be modified to fulfill the requirement of different applications ranging from automotive and aircraft industry to sports and leisure. The development work related to aluminum/aluminium alloy matrix composites is currently focused on following two sectors:

(i) Continuous fiber reinforced composite with superior properties for every specific applications.

(ii) Mass production technologies of inexpensive discontinuously reinforced composites with moderate properties for wider range of applications.

1.4.1 Properties of Aluminium based MMCs

The salient properties of aluminium based MMCs are [2]:

a) Specific Stiffness
b) Specific Strength
c) Fatigue Resistance
d) Coefficient of Thermal Expansion
e) Wear Resistance

a) Specific Stiffness

The addition of stiff metallic or ceramic reinforcement materials to the metal matrix results in an increase in elastic modulus of the composites materials. In case of light weight metals, such as aluminium, titanium and magnesium, the increase can be very significant even at moderate levels of reinforcement addition.

b) Specific Strength

In addition to high stiffness, aluminium based MMCs also possess high strength. The strength of the composite is strongly dependent on the specific characteristics of the reinforcement material, its morphology and the type of bonding at reinforcement-matrix interface. Continuous fiber reinforced composites exhibit high specific strength levels in the direction of the fiber orientation.

c) Fatigue Resistance

The addition of reinforcement in aluminium/aluminium alloy matrix significantly affects its fatigue resistance. The mechanisms of fatigue resistance enhancement differ in composites depending on the morphology of the reinforcement and characteristics of reinforcement-matrix interface.

d) Coefficient of Thermal Expansion (CTE)

The typical ceramic reinforcements for MMCs have significantly lower values of the coefficient of thermal expansion (CTE) than the metal matrix into which they are incorporated. Thus, the addition of ceramic reinforcement to the high expansion metals such as aluminium, magnesium, copper, and titanium can result in substantial reduction in the CTE.

(e) Wear Resistance

The high hardness of the typical ceramic reinforcement materials can also affect the tribological properties of the metal matrix composites compared to pure matrix. Particulate reinforced MMCs have been of particular interest for use in wear resistance dominated applications.

1.4.2 Typical application of Discontinuously Reinforced Aluminium Matrix Composite (DRAMCs)

Discontinuously reinforced aluminium matrix composites (DRAMCs) are widely used in various applications as discussed below [3].

(i) Aircraft

A significant portion of aircraft structure is designed by stiffness so as a result many of the aircraft structural applications for MMCs seek to capitalize on the increased specific stiffness provided by aluminium based MMCs. Aircraft structural applications actually require a combination of properties including adequate strength, damage tolerance and corrosion resistance. MMCs have lower damage tolerance properties compared to pure metal matrix. Silicon carbide particle reinforced aluminium MMC have been used in the US AIR Force F-16 Aircraft.

(ii) Aero-Engine

Aluminium based MMCs have been used in aero engines, especially in the area of fan exit guide vanes. In this application, both specific stiffness and specific strength, especially at elevated temperature, are the critical properties. Similar to aircraft structure, other properties, including fatigue, creep and oxidation resistance, are also very important in these applications.

(iii) Brake System

Aluminium based MMCs offer a very useful combination of properties for braking systems and have therefore replaced the conventional material such as cast iron. Specially, the wear resistance and high thermal conductivity of aluminium based MMCs enable substitution of cast iron in disk brake rotors and brake drums with an attendant weight saving of the order of 50-60%. This helps in reducing inertia force and thereby providing additional benefits. The light weight MMCs rotor also provides increased acceleration and reduced braking distance.

(iv) Other Automotive Applications

MMCs based on Aluminium matrices, are candidates for application in automotive sector. Typical automotive applications are listed in Table-1.

Table 1: Typical Application of MMCs in Automobile Sector [2]

Products	MMCs System	Characteristics of applied MMCs	Year(Maker)
Vane, Pressure side plate of oil pressure vane pump	Al_2O_3- SiO_2	Wear Resistance	1987(Hiroshima Aluminium)
Ring,Groove Reinforced Piston	Al_2O_3/Al-alloy	Light weight, Wear resistance at elevated temperature	1983(Toyota)
Shock absorber	SiC_P/Al-alloy	Light weight, Wear resistance, Thermal diffusivity	1989(Mitsubishi Aluminium)
Bicycle frame	SiC_W/6061	Light weight, High specific rigidity	1989(Kobe steel)
Diesel engine piston	SiC_W/Al-alloy	Light weight,Wear Resistance	1989(Niigata)

1.5 Limitation of Composites

a) High cost of fabrication of composite materials. For example, a part made-up of graphite/epoxy composite may cost up to 10 to 15 times of materials cost.
b) Mechanical characterization of composite structure is more complex than that of a metal structure. Composite materials are not isotropic (i.e. do not possess same properties in all the direction). For example, a single layer of graphite/epoxy composite requires nine stiffness and strength constants for conducting mechanical analysis while in the case of steel only four stiffness and strength constant are required.
c) Repair of composite is not a simple process as compared to metals.
d) Composites do not have good combination of strength and fracture toughness as compared to metals.

e) Composites do not necessarily give higher performance in the all the property used for material selection.

CHAPTER 2

LITERATURE REVIEW

In most of the engineering and structural applications a component made of composite materials has to operate under severe thermo-mechanical loading where creep becomes significant. Therefore, the present investigation deals with the creep behavior of composite materials. The prediction and analysis of creep properties for the assessment of service life of the components made of composite materials, is of great practical importance for practicing engineers in order to save time and avoid errors, since the performance evaluation of real life components under multi-axial stress condition is quite complex and very time consuming.

2.1 Creep

The progressive deformation of a material at constant load is called creep. To determine the engineering creep curve of a metal, a constant load is applied to a standard specimen maintained at a constant temperature and the strain (extension) is determined as a function of time.

Curve A in the Fig.2.1 illustrates the idealized shape of the creep curve. The slope of this curve ($d\varepsilon/dt$) is referred to as the creep rate ($\dot{\varepsilon}$). A typical creep curve exhibits three stages as evident from Fig.2.1. These stages are readily distinguishable and depend strongly on the applied stress and temperature.

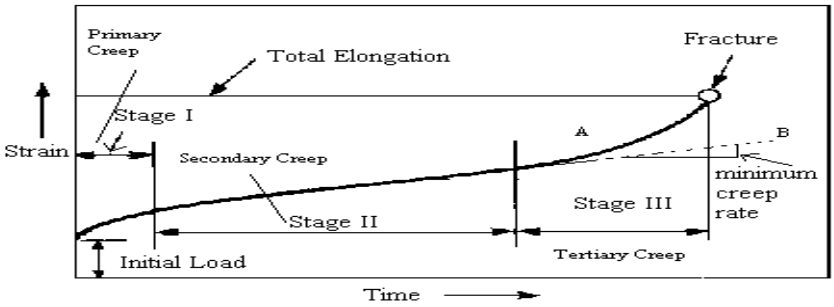

Fig.2.1 Creep curve showing the three steps of creep.
(Curve A: Constant curve load; Curve B: Constant stress curve)

The first stage of the creep, known as primary creep, represents a region of decreasing creep rate. Primary creep is a period of predominantly transient creep in which the resistance of the material increases by virtue of its own deformation. Primary creep occurs at low temperature and low stress levels.

The second stage of creep, also known as secondary creep, is a period of nearly constant creep rate which results from a balance between the competing processes of strain hardening and recovery. For this reason, secondary creep is usually referred to as Steady State Creep. The average value of the creep rate during secondary creep is called the minimum creep rate.

Third stage or tertiary creep mainly occurs in constant load creep tests at high stresses and high temperature. Tertiary creep occurs when there is an effective reduction in cross-sectional area either because of necking or internal void formation. Third stage creep is

often associated with metallurgical changes such as coarsening of precipitate particles, recrystallization or diffusional changes in the phases present.

The dashed line (Curve B) in Fig.2.1 shows the shape of a constant-stress creep curve. In engineering situations, it is usually the load, not the stress that is maintained constant, so a constant load creep test is more important [4].

Garofalo [4] has proposed that the creep curve can be represented by the following equation for a limited number of materials:

$$\varepsilon = \varepsilon_0 + \varepsilon_t(1 - e^{-rt}) + \dot{\varepsilon}$$

where, ε is total strain, ε_0 is the instantaneous strain on loading, ε_t is the limit for transient creep, r is the ratio of transient creep rate to the transient creep strain, and $\dot{\varepsilon}$ is the steady state creep rate.

2.2 Yield Criteria for Ductile Materials

The problem of deducing mathematical relationships for predicting the conditions at which plastic yielding begins when a material is subjected to any possible combination of stress is an important consideration in the field of plasticity. In uniaxial loading, as in a tension test, macroscopic plastic flow begins at the yield stress σ_y. It is expected that yielding under a situation of combined stresses can be related to some particular combination of principal stresses. Since this work deals with the creep in aluminium based MMCs which are ductile in nature therefore, the yield criteria applicable for ductile materials have been discussed in this section.

2.2.1 Distortion Energy Criterion (Von Mises Criterion)

The criteria for predicting the onset of yielding in ductile metals is Von Mises or, Distortion-Energy Criterion [4].Von Mises has proposed that yielding would occur when the second invariant of the stress deviator J_2 exceeds some critical value.

$$J_2 = \frac{1}{6}\left[(\sigma_1-\sigma_2)^2 + (\sigma_2-\sigma_3)^2 + (\sigma_3-\sigma_1)^2\right] = k^2 \quad \ldots\ldots\ldots\ldots\ldots\ldots\ldots\ldots\ldots\ldots (1)$$

To evaluate the constant *k* and relate it to yielding in the tension test, it is realized that at yielding in uniaxial tension $\sigma_1=\sigma_y$, $\sigma_2=\sigma_3=0$. Therefore,

$$\sigma_y^2+\sigma_y^2=6k^2$$

$$\sigma_y=\sqrt{3}k \quad \text{.....(2)}$$

Substituting Eq. (2) in Eq. (1) one gets the usual form of the Von Mises yield criterion as given below,

$$\sigma_y=\frac{1}{\sqrt{2}}[(\sigma_1-\sigma_2)^2+(\sigma_2-\sigma_3)^2+(\sigma_3-\sigma_1)^2]^{1/2} \quad \text{.....(3)}$$

2.2.2 Maximum Shear Stress Criterion (Tresa Yield Criterion)

This yield criterion assumes that yielding occurs when the maximum shear stress reaches the value of the shear stress in the uniaxial tension test. The maximum shear stress [4] is given by,

$$\tau_{\max}=(\sigma_1-\sigma_3)/2 \quad \text{..... (4)}$$

where, σ_1 is the algebraically largest and σ_3 is the algebraically smallest principal stress.

For uniaxial tension, $\sigma_1=\sigma_y$, $\sigma_2=\sigma_3=0$ and the shearing yield stress τ_y is equal to $\sigma_y/2$. Therefore, Eq. (4) becomes,

$$\tau_{\max}=(\sigma_1-\sigma_3)/2=\sigma_y/2 \quad \text{..... (5)}$$

Therefore, the maximum shear stress criterion is given by

$$\sigma_1-\sigma_3=\sigma_y \quad \text{..... (6)}$$

The maximum shear stress criterion is mathematically less complicated than the Von Mises criterion [4], and for this reason it is often used in engineering design. Fig.2.2 shows graphical comparison of Von Mises and Tresa Yield criteria.

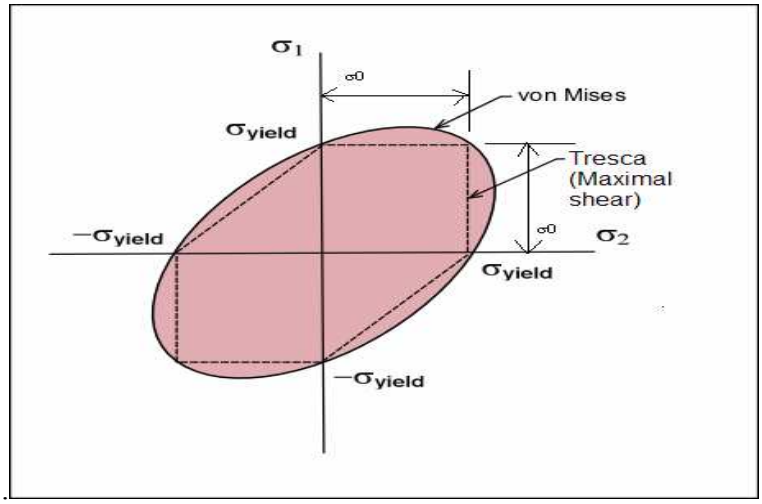

Fig.2.2. Comparison of Von Mises and Tresca Criterion

2.2.3 Hill Anisotropy Criterion

The yield criteria considered so far assumes that the material is isotropic. While this may be the case at the start of plastic deformation, it certainly is no longer a valid assumption after the metal has undergone appreciable plastic deformation. Moreover, most fabricated metal shapes have anisotropic properties, so that it is likely that the tubular specimens used for basic studies of yield criteria incorporate some degree of anisotropy. Certainly the Von Mises criterion as given by Eq. (3) would not be valid for a highly oriented cold-rolled sheet or a fiber–reinforced composite material.

Hill [4] has formulated the Von Mises yield criterion for an anisotropic material having orthotropic symmetry as given below,

$$F(\sigma_y - \sigma_z)^2 + G(\sigma_z - \sigma_x)^2 + H(\sigma_x - \sigma_y)^2 + 2L\tau_{yz}^{\ 2} + 2M\tau_{zx}^{\ 2} + 2N\tau_{xy}^{\ 2} = 1 \ldots\ldots\ldots (7)$$

where, σ_x, σ_y and σ_z are normal stresses along x, y and z directions respectively. τ_{yz}, τ_{zx}, τ_{xy} are shear stresses and F, G, H, L, M and N are constants defining the degree of anisotropy. For principal axes of orthographic symmetry, the above equation reduces to following form,

$$F(\sigma_y-\sigma_z)^2+G(\sigma_z-\sigma_x)^2+H(\sigma_x-\sigma_y)^2=1 \quad \ldots\ldots (8)$$

If x, y and z are the yield stresses in the principal direction 1, 2, 3 respectively, then by substituting in Eq. (8), the anisotropic constants may be evaluated as,

$$G+H=\frac{1}{x^2}$$

$$H+F=\frac{1}{y^2} \quad \ldots\ldots (9)$$

$$F+G=\frac{1}{z^2}$$

The Hill criterion reduces to Von Mises criterion if the yield stress x, y and z are equal. In other words, when the anisotropic constants appearing in Hill criterion are set equal (i.e. $F=G=H=\frac{1}{2x^2}$) the Hill criterion reduces to Von Mises criterion.

2.2.4 Hoffman Yield Criterion

Hoffman has proposed a fracture condition for orthotropic brittle materials using nine material parameters, which accounts for the different yield strength under compression and tension in various directions [5]. The condition has been subsequently used as a yield criterion for anisotropic materials by various investigators. In its original form, the Hoffman criterion takes anisotropy also into account and could be stated in terms of principal stresses as,

$$C_1(\sigma_{22}-\sigma_{23})^2+C_2(\sigma_{33}-\sigma_{11})^2+C_3(\sigma_{11}-\sigma_{22})^2)+C_4\sigma_{11}+C_5\sigma_{22}+C_6\sigma_{33}+C_7\sigma_{23}^2+C_8\sigma_{31}^2+$$

$$C_9\sigma_{12}^2-1=0 \quad (10)$$

In the principal stress space, the criterion simplifies to,

$$C_1(\sigma_{22}-\sigma_{23})^2+C_2(\sigma_{33}-\sigma_{11})^2+C_3(\sigma_{11}-\sigma_{22})^2)+C_4\sigma_{11}+C_5\sigma_{22}+C_6\sigma_{33}-1=0 \quad \ldots\ldots (11)$$

The Hoffman Yield Criterion has been developed by borrowing feature from Von Mises isotropic yield condition and Hill anisotropic yield criterion. This criterion reduces to Hill criterion [5] by setting $C_4=C_5=C_6=0$, in Eq. (11). When in Eq. (11) $C_1=C_2=C_3$ and,

$C_4=C_5=C_6=0$, the criterion reduces to Von Mises yield surface in the principal stress space [4].

2.3 Creep Laws

In order to correlate effective stress to effective strain rate various laws have been propose by several investigators. Norton [6] has proposed that effective strain (ε) is related to applied stress (σ) by a power law relation of the following form:

$$\dot{\bar{\varepsilon}} = A\sigma^{n_a} \exp(-Q_a / RT)$$

where, $\dot{\bar{\varepsilon}}$ is the steady state creep rate, A is the constant sensitive to microstructure, σ is the applied stress, n_a is the apparent stress exponent, Q_a is the apparent activation energy, R is the gas constant and T is the absolute temperature. Norton's law has been widely criticized because of following two reasons [6]:

Firstly, the stress dependence of the creep rate, as described by the value of the stress exponent, n_a, is anomalously high and ranges from about 10 to 75.

Secondly the temperature dependence of the creep rate measured in terms of creep activation energy, Q_a, is often much larger than that for lattice self-diffusion.

In order to rationalize the strong stress and temperature dependency of creep rate reported for the discontinuously reinforced aluminium matrix composites, the concept of an effective stress has been developed. In this respect the Norton's power law creep equation as given above can be modified as,

$$\dot{\bar{\varepsilon}} = A'[(\bar{\sigma} - \sigma_0) / E]^n \exp(-Q / RT)$$

where $\dot{\bar{\varepsilon}}$ is the effective creep rate, A' is the structure dependent parameters, $\bar{\sigma}$ is the applied stress , σ_0 is the threshold stress, n is the true stress exponent, E is the temperature-dependent Young's Modulus, Q is the true activation energy, R is the gas constant and T is the absolute temperature.

It has been pointed out that the creep behavior of aluminium alloys and their composites is related to modified creep behavior of solid solution alloys [6]. Thus, the equation developed for solid solution alloys can be used to describe the creep behavior of

composites provided that the applied stress is replaced by an effective stress. The true stress exponent n is usually selected as 3, 5 and 8. These values of n correspond to three well-documented creep cases for metal and alloys: n=3 for creep controlled by viscous glide processes of dislocation, n=5 for creep controlled by high-temperature dislocation climb and n=8 for lattice diffusion-controlled creep with a constant structure [6].

2.4 Constitutive Equations for Creep under Multiaxial Loading

In real life applications, most of the engineering components such as rotating disc, rotating cylinders etc., undergoing creep are subjected to multi-axial stress condition. The treatment for multiaxial creep in isotropic material begin with well-known Levy-Mises equation [5] in principal stress space as given below,

$$d\varepsilon_1=\frac{d\bar{\varepsilon}}{\bar{\sigma}}[\sigma_1-(\sigma_2+\sigma_3)/2]$$

$$d\varepsilon_2=\frac{d\bar{\varepsilon}}{\bar{\sigma}}[\sigma_2-(\sigma_1+\sigma_3)/2] \quad \text{.....(12)}$$

$$d\varepsilon_3=\frac{d\bar{\varepsilon}}{\bar{\sigma}}[\sigma_3-(\sigma_1+\sigma_2)/2]$$

where, $d\varepsilon_1$, $d\varepsilon_2$ and $d\varepsilon_3$ indicate increments of plastic strain components, $\bar{\sigma}$ is the effective stress and $d\bar{\varepsilon}$ is the effective strain increments.

The effective stress, $\bar{\sigma}$ and strain increment, $d\bar{\varepsilon}$, are given by,

$$\bar{\sigma}=\frac{1}{\sqrt{2}}[(\sigma_2-\sigma_3)^2+(\sigma_3-\sigma_2)^2+(\sigma_1-\sigma_2)^2]^{1/2}$$

$$d\varepsilon=\frac{\sqrt{2}}{3}[(d\varepsilon_1-d\varepsilon_2)^2+(d\varepsilon_2-d\varepsilon_3)^2+(d\varepsilon_3-d\varepsilon_1)^2]^{1/2}$$

Replacing the strain increments by strain rates in Eq. (12) to obtain,

$$\dot{\varepsilon}_1=\frac{\bar{\varepsilon}}{\bar{\sigma}}[\sigma_1-(\sigma_2+\sigma_3)/2]$$

$$\dot{\varepsilon}_2=\frac{\bar{\varepsilon}}{\bar{\sigma}}[\sigma_2-(\sigma_1+\sigma_3)/2] \quad \text{.....(13)}$$

$$\acute{\varepsilon}_3 = \frac{\bar{\varepsilon}}{\bar{\sigma}} [\sigma_3 - (\sigma_1 + \sigma_2)/2]$$

The set of Eqs. (13) are known as the constitutive equations for creep in an isotropic material in principal stress space.

2.5 Cylinder and Creep

Cylinder has almost unlimited applications such as pressure vessels, fuel tanks, accumulator shells, paintball cylinders, emergency breathing cylinders, cylinders for aerospace industries and military applications, composite rotors (flywheel) etc. In some of these applications such as pressure vessel for industrial gases or a media transportation of high pressurized fluids and composite rotors (flywheel), it is subjected to severe mechanical and thermal loadings resulting in significant creep which may lead to reducing service life. The excellent creep resistance along with high specific strength offered by aluminium/aluminium alloy based MMCs make them a suitable choice for such applications. Numerous investigators have carried out creep analysis in a cylinder as discussed below.

Davis *et al* [7] have studied plastic deformation of a hollow thick-walled cylinder and have suggested that for a perfectly plastic material the solution directly gives the steady-state creep solution also.

Rimrott [8] has used generally accepted assumption of constant density, zero axial strain and distortion energy law and derived equation for creep rates, strains and stresses of a thick-walled, closed end, circular hollow cylinder under internal pressure. Cylinder is made of an isotropic homogeneous material. The strains are considered large and finite strain theory is used. A known creep rate versus stress relation is then used to solve a specific problem.

Danilova [9] has discussed the stress distribution in a rotor during non-steady creep, **Rabotnov [10, 11]** have also studied non-steady creep in rotating solid and hollow cylinders. The analyses have assumed that the material is isotropic and remains so during creep.

Dipti Dev [12] has obtained the solution for rotating hollow cylinder considering infinitesimal strains, isotropic yield criterion, creep-strain law and assuming

incompressible material.

Bhatnagar and Arya [13] have used finite strain theory to study creep behavior of pressurized (internal, internal and external both) thick-walled cylinder made of anisotropic material under large strains. The anisotropy is observed to have significant effect on the axial stress, strain and strain rate.

Arya *et al* [14] have used large strain theory to analyze the effect of the material anisotropy on the creep of the pressurized thick-walled spherical vessel. It is found that the creep strain varies with varying anisotropy of material. The comparison of results obtained for the anisotropic case with those obtained for the isotropic case shows that the stress and strain distribution in the wall of vessel is strikingly different for two cases.

Bhatnagar *et al* [15] have analyzed the stress and strain rate distributions in a hollow thick circular cylinder rotating about its own axis with constant angular speed. The cylinder is assumed to be made of a homogeneous and orthotropic material. The steady state creep is described by Norton's law. The effect of anisotropy and stress exponent n in the creep law has been studied. It is concluded that the stress and strain-rate distributions are significantly affected by the anisotropy of material and the value of exponent n. The study also reveals that the value of the effective stress for an anisotropic material for which the ratios of axial to the tangential strain rate and of radial to tangential strain rate are equal to 1.2, are lower than the corresponding values for an isotropic material for which these ratio are 1.0. Due to power law between effective strain rate and effective stress, much lower values of the effective strain rate for the foregoing anisotropic material is obtained than those obtained for the isotropic material. The study concludes that anisotropic material may be beneficial for the manufacture of the cylinders because of longer life and ability to sustain larger forces without a risk of failure under creep.

Gupta and Dharmani [16] have used Seth's transition theory to derive creep stress equations in transversely isotropic rotating hollow and solid circular cylinders. Their results are found to be same as those of Rimrott and Luke [11] and Dipti Dev [13] derived by assuming Von-Mises Yield condition and Norton's laws.

Hulsurkar [17] has applied Seth's transition theory of elastic-plastic and creep deformations to the problem of creep in composite cylinders under uniform internal pressure. The expressions for transitional stresses in creep are obtained in a general form

which, as a special case, reduces to those derived by assuming the creep laws.

Arya *et al* [18] have investigated creep in a thin circular cylindrical shell made of a homogeneous, incompressible and orthotropic material using a non steady creep law. The result indicate that material anisotropy could be exploited to provide a better shell design yielding lower strains and longer service life for the shell.

Rimrott [19] has presented creep analysis of rotating isotropic cylinder considering finite strain theory. The appropriate solution has been obtained for large strain.

Bhatnagar *et al* [20] have analyzed creep in a thick walled orthotropic rotating cylinder. It is observed that material anisotropy may have beneficial effect on stress and strain rate distributions. The result obtained using small strain theory is found to be on unsafe side when compared to those obtained using finite strain theory.

Bhatnagar *et al* [21] have presented the analysis for an orthotropic thick-walled cylinder undergoing creep due to the combined action of internal and external pressure, and rotary inertia. It is observed that the material stronger in radial direction may be beneficial for the design of the cylinder due to lower effective stress.

Gupta and Pathak [22] have also used Seth's transition theory to obtain creep stresses and strain rates in a thick walled circular cylinder made of compressible/incompressible materials under internal pressure. It is noticed that the circumferential stress has maximum value at the external surface of the cylinder made of incompressible material as compared to compressible material. Introduction of thermal effects is observed to reduce the stresses at external surface of the cylinder in comparison to pressure effects only. Strain rates are found to be maximum at internal surface of the cylinder made of compressible material and tend to decrease with radius. With the introduction of thermal effects, the creep rates are found to increase more at the internal surface than at the external surface, when compared to a cylinder subjected to pressure only.

Tzeng [23] has developed a viscoelastic analysis to investigate the creep and stress relaxation in a multilayered composite cylinder subjected to rotation. The analysis accounts for layer-by-layer variation of material properties, composite fiber orientations, temperature and density gradients through thickness of cylinders. A closed form solution based on the corresponding elastic problem is derived for a generalized plane strain state in a thick-walled multilayered cylinder. A Laplace transformation is then applied to

obtain the numerical solution of viscoelastic problem.

CHAPTER 3

PROBLEM FORMULATION

Creep analysis of rotating cylinder subjected to elevated temperature has been the subject of numerous investigations. In most of the studies the cylinder material is assumed to be monolithic and only very limited studies deal with the behavior of a rotating cylinder made of composite material. The efforts have been made to develop mathematical models to evaluate creep response of a rotating cylinder. The excellent mechanical properties like high specific strength and stiffness, and high temperature stability offered by aluminium/aluminium alloy based composites consisting of ceramic reinforcement (e.g. Sic) make them appropriate choice for use in severe thermo-mechanical loading conditions as observed in some of the applications of rotating cylinders.

Further, the creep performance of engineering components such as rotating disc made of composites can be significantly improved by modifying the materials parameters like reinforcement size, shape and content, and the temperature of application [24].

In the light of above said it is decided to investigate effect of material parameters on the steady-state creep behavior of a rotating thick cylinder made of Al-SiC_p.

The following objectives are set for the present work:

- Develop a mathematical model to evaluate steady state creep response of rotating cylinder made of light weight Al-SiC_P composite.
- Development of computer code to calculate stresses and strain rates in cylinder.
- Investigate the effect of reinforcement (SiC_P) size and content, and operating temperature on the creep behavior of rotating cylinder.

CHAPTER 4

ANALYSIS OF CREEP BEHAVIOR

In order to investigate the effect of material parameters on the steady state creep performance of a hollow rotating cylinder, Fig. 4.1, a mathematical model is developed in this chapter. The model will be used to calculate stress and strain-rate distributions in the wall of a hollow thick-walled circular cylinder, rotating about its own axis with a constant angular speed. The cylinder is assumed to be made of Al-SiCp.

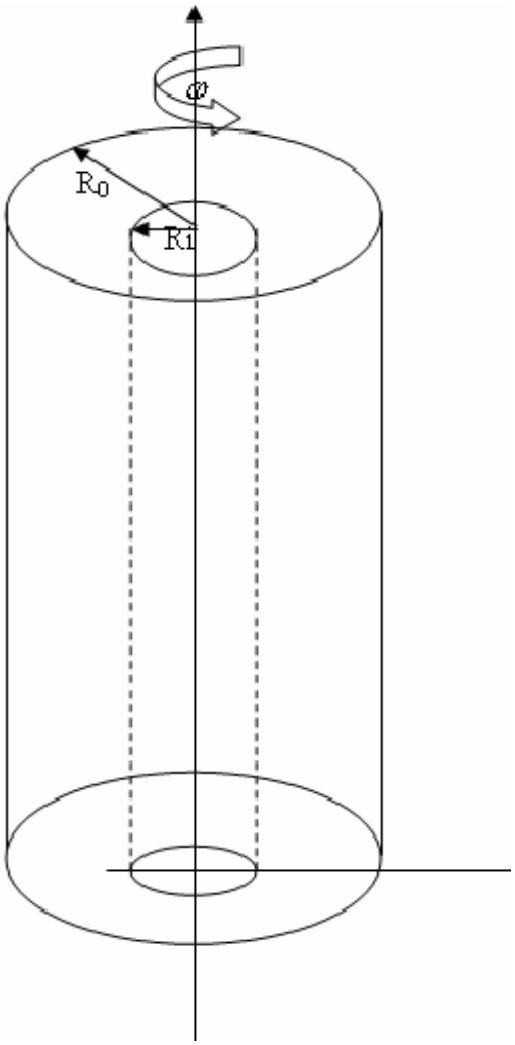

Fig. 4.1: Thick Walled Cylinder rotating with an angular speed ω about its own axis.

Consider a thick-walled cylinder rotating about its axis with a constant angular speed ω. Let ρ be the density of material and r_i and r_o, be inner and outer radii of cylinder.

4.1 Fundamental Relations

The equation of equilibrium for a rotating cylinder is given by the relation [15]:

$$r \, d\sigma_r / dr = (\sigma_\theta - \sigma_r) - \rho\omega^2 r^2 \quad \ldots\ldots (1)$$

It is assumed that the creep deformation does not involve appreciable volume changes thus…

$$\dot{\varepsilon}_r + \dot{\varepsilon}_\theta + \dot{\varepsilon}_z = 0 \quad \ldots\ldots (2)$$

If the cylinder is constrained from contracting in axial direction, then...

$$\dot{\varepsilon}_z = 0 \quad \ldots\ldots (3)$$

Therefore, Eqn. (2) reduces to ……………

$$\dot{\varepsilon}_r + \dot{\varepsilon}_\theta = 0 \quad \ldots\ldots (4)$$

The material of ther disc (i.e. Al-SiCP) is assumed to undergo steady state creep following Sherby's Law as given by following equation

$$\dot{\varepsilon} = A'[(\bar{\sigma} - \sigma_0)/E]^n \exp(-Q/RT)$$

The above equation can be alternatively written as:

$$\dot{\varepsilon} = [\mathrm{M}\,(\sigma_e - \sigma_o)]^n \quad \ldots\ldots (5)$$

where, $M = \frac{1}{E}\left(\frac{AD_L\lambda^3}{|b_r|^5}\right)^{1/8}$ and σ_o is the threshold stress and are known as the creep parameters. The parameters M and σ_o depend on the reinforcement size, *P*, and the percentage of dispersed particles (SiCP), *V*, apart from the temperature of application, *T*. The values of M and σ_o in terms of material variables *P* and *V* and operating temperature, *T*, have been extracted by using Sherby's law to describe the creep results obtained by Pandey *et al* [25] for Al–SiCP composites under uniaxial loading as reported in Table-1. The procedure of obtaining these parameters is described elsewhere [24].

Table-1: Values of Creep Constants based on Experimental Results [25]

Particle Size $P\ (\mu m)$	Temperature $T\ (K)$	Particle Content $V\ (vol\%)$	Mx10^{-4} $(s^{-1/8}/MPa)$	σ_0 (MPa)
1.7	623	30	51.8	34.57
14.5			74.7	34.12
45.9			94.9	33.02
1.7	623	10	96.3	15.24
		20	59.4	24.83
		30	51.8	34.32
1.7	623	20	59.4	24.83
	673		89.7	24.74
	723		129.5	25.72

The constitutive equations for creep in a rotating cylinder under multiaxial state of stress as given by Bhatnagar *et al* [15] may be written as:

$$\dot{\varepsilon}_r = \frac{\dot{\varepsilon}}{2\sigma_e}[(G+H)\sigma_r - F\sigma_\theta - H\sigma_z]$$

$$\dot{\varepsilon}_\theta = \frac{\dot{\varepsilon}}{2\sigma_e}[(H+F)\sigma_\theta - F\sigma_z - H\sigma_r]$$

$$\dot{\varepsilon}_z = \frac{\dot{\varepsilon}}{2\sigma_e}[(F+G)\sigma_z - G\sigma_r - F\sigma_\theta]$$

Using Eqn. (5) into above equations:

$$\dot{\varepsilon}_r = \frac{[M(\sigma_e - \sigma_0)]^n}{2\sigma_e}[(G+H)\sigma_r - H\sigma_\theta - G\sigma_z]$$

$$\dot{\varepsilon}_\theta = \frac{[M(\sigma_e - \sigma_0)]^n}{2\sigma_e}[(H+F)\sigma_\theta - F\sigma_z - H\sigma_r] \quad \ldots\ldots\ldots\ldots\ldots (6)$$

$$\dot{\varepsilon}_z = \frac{[M(\sigma_e - \sigma_0)]^n}{2\sigma_e}[(F+G)\sigma_z - G\sigma_r - F\sigma_\theta]$$

The effective stress, σ_e, is given by Hill anisotropic yield criterion as given by…

$$\sigma_e = \frac{1}{\sqrt{G+H}}[H(\sigma_\theta - \sigma_r)^2 + G(\sigma_r - \sigma_z)^2 + F(\sigma_z - \sigma_\theta)^2]^{1/2} \ldots. (7)$$

It is important to mention that the disc material (Al-SiC_P) is assumed to be isotropic and follows Von Mises isotropic yield criterion, which can be obtained by setting $F=G=H$ in the Hill anisotropic yield criterion as given by Eqn. (7).

The present analysis assumes that ε_Z=0, therefore the last equation amongst the set of Eqs. (7) yields:

$$0 = \frac{[M(\sigma_e - \sigma_0)]^n}{2\sigma_e}\ [(F+G)\sigma_z - G\sigma_r - F\sigma_\theta]$$

The above equation implies that either…

$$\sigma_e = \sigma_0$$

i.e. Means effective stress= threshold stress, which can not be possible.

or

$$[(F+G)\sigma_z - G\sigma_r - F\sigma_\theta] = 0$$

i.e. $$\sigma_z = \frac{G\sigma_r + F\sigma_\theta}{(F+G)} \ldots\ldots\ldots\ldots\ldots\ldots\ldots\ldots\ldots\ldots (8)$$

Substituting the value of σ_z from Eqn. (8) into second equation amongst set of constitutive Eqs. (6) and simplifying, one gets...

$$\dot{\varepsilon}_\theta = \frac{[FG+GH+HF]}{2(F+G)} \times \frac{[M(\sigma_e - \sigma_0)]^n}{\sigma_e} \times (\sigma_\theta - \sigma_r) \qquad (9a)$$

Writing Eqn. (7) again

$$\sigma_e = \frac{1}{\sqrt{G+H}}[H(\sigma_\theta - \sigma_r)^2 + A + B]^{1/2} \qquad (10)$$

Where, A= $G(\sigma_r - \sigma_z)^2$ and B= $F(\sigma_z - \sigma_\theta)^2$.

Substituting σ_Z from Eqn. (8), the values of A and B can be obtained as:

$$\text{A} = GF^2\ \frac{GF^2}{(F+G)^2}(\sigma_\theta - \sigma_r)^2$$

$$\text{B} = \frac{FG^2}{(F+G)}(\sigma_\theta - \sigma_r)^2$$

Therefore, Eqn. (10) becomes:

$$\sigma_e = \frac{1}{\sqrt{G+H}}[H(\sigma_\theta - \sigma_r)^2 + \frac{GF^2}{(F+G)^2}(\sigma_\theta - \sigma_r)^2 + \frac{FG^2}{(F+G)^2}(\sigma_\theta - \sigma_r)^2]^{\frac{1}{2}}$$

Above equation can be further simplified to:

$$\sigma_e = \left[\frac{FG+GH+HF}{(G+H)\times(F+G)}\right]^{\frac{1}{2}} \times (\sigma_\theta - \sigma_r) \tag{11}$$

On substituting σ_e from Eqn. (11) into second equation amongst set of Eqs. (6), one may obtain:

$$\dot{\varepsilon_\theta} = \frac{[M(\sigma_e - \sigma_0)]^n}{2} \times \left[\frac{(FG+GH+HF)\times(G+H)}{(F+G)}\right]^{\frac{1}{2}}$$

or,

$$\dot{\varepsilon} = (\sigma_e - \sigma_0)^n \times P_1 \tag{12}$$

where

$$P_1 = \frac{M^n}{2} \times \left[\frac{(FG+GH+HF)\times(G+H)}{(F+G)}\right]^{\frac{1}{2}} \tag{13}$$

Eqn. (12) can be also written as:

$$\sigma_e = (\frac{\dot{\varepsilon_\theta}}{P_1})^{\frac{1}{2}} + \sigma_0 \tag{14}$$

Substituting σ_e from Eqn. (11) into Eqn. (14), one gets,

$$P_2 \times (\sigma_\theta - \sigma_r) = (\frac{\dot{\varepsilon_\theta}}{P_1})^{\frac{1}{n}} + \sigma_0 \tag{15}$$

where

$$P_2 = \left[\frac{FG+GH+HF}{(G+H)\times(F+G)}\right]^{\frac{1}{2}} \quad \text{(Constant)} \tag{16}$$

Eqn. (15) may be rearranged to obtain:

$$(\sigma_\theta - \sigma_r) = \left(\frac{\dot{\varepsilon_\theta}}{k}\right)^{\frac{1}{n}} + \frac{\sigma_0}{P_2} \tag{17}$$

where $k = P_1.P_2^{\,n}$, a constant.

Substituting P_1 and P_2 from Eqs. (13) and (16), the constant k may be obtained as,

$$k = \frac{M^n}{2} \times \left[\frac{FG + GH + HF}{(F+G)} \right]^{\frac{n+1}{2}} \times \frac{1}{(G+H)^{\frac{n-1}{2}}} \tag{18}$$

Let u is radial displacement at any radius r, then the strain rates in radial and tangential direction is given as:

$$\dot{\varepsilon}_r = \frac{d\dot{u}}{dr} \tag{19}$$

$$\dot{\varepsilon}_\theta = \frac{\dot{u}}{r} \tag{20}$$

Differentiating Eqn. (20) w.r.t. r, one may get:

$$\frac{d\dot{\varepsilon}_\theta}{dr} = \frac{1}{r}\frac{d\dot{u}}{dr} - \frac{\dot{u}}{r^2}$$

The above equation can be further simplified as:

$$r\frac{d\dot{\varepsilon}_\theta}{dr} = \dot{\varepsilon}_r - \dot{\varepsilon}_\theta \tag{21}$$

Substituting $\dot{\varepsilon}_r = -\dot{\varepsilon}_\theta$ from Eqn. (4) into Eqn. (21) one may write:

$$\frac{1}{\dot{\varepsilon}_\theta} d\dot{\varepsilon}_\theta = -2\frac{dr}{r}$$

On integrating above equation:

$$\int \frac{1}{\dot{\varepsilon}_\theta} d\dot{\varepsilon}_\theta = -2\int \frac{1}{r} dr$$

or

$$\ell n\, \dot{\varepsilon}_\theta = -2\ell nr + c_1$$

or

$$\dot{\varepsilon}_\theta = \frac{c_1}{r^2} \tag{22}$$

where c_1 is a constant of integration.

Substituting value of $\dot{\varepsilon}_\theta$ from Eqn. (22) into Eqn. (17):

$$(\sigma_\theta - \sigma_r) = \left(\frac{c_1}{kr^2}\right)^{\frac{1}{n}} + \frac{\sigma_0}{P_2}$$

or

$$(\sigma_\theta - \sigma_r) = \frac{c_2}{r^{\frac{2}{n}}} + \frac{\sigma_0}{P_2} \tag{23}$$

where $c_2 = \frac{c_1}{k^{\frac{1}{n}}}$ is another constant.

Putting value of $(\sigma_\theta - \sigma_r)$ from Eqn. (23) into equilibrium Eqn. (1), we get:

$$r\frac{d\sigma_r}{dr} = \frac{c_2}{r^{\frac{2}{n}}} + \frac{\sigma_0}{P_2} - \rho\omega^2 r^2$$

or

$$d\sigma_r = \frac{c_2}{r^{\frac{2+n}{n}}}dr + \frac{\sigma_0}{p_2.r}dr - \frac{\rho\omega^2 r^2}{r}dr$$

On integrating above equation one may get:

$$\sigma_r = -\frac{c_2}{2} \times \frac{n}{r^{\frac{2}{n}}} + \frac{\sigma_0}{P_2}\ell nr - \frac{\rho\omega^2 r^2}{2} + c_3 \tag{24}$$

where c_3 is another constant of integration.

In case of a free rotating orthotropic hollow cylinder the radial stress, σ_r, must zero at the inner and the outer radii of the cylinder, thus

$$\begin{pmatrix} \sigma_r = 0 \ at \ r = r_i \\ \sigma_r = 0 \ at \ r = r_o \end{pmatrix} \tag{25}$$

The constants c_1 and c_2 defined above may be obtained by applying the boundary conditions given by Eqn. (25) into Eqn. (24).

Therefore, at $r=r_o$, Eqn. (24) becomes:

$$\frac{c_2}{2} \times \frac{n}{r_o^{\frac{2}{n}}} = \frac{\sigma_0}{P_2}\ell n.r_o - \frac{\rho\omega^2 r_o^{\ 2}}{2} + c_3 \tag{26}$$

Similarly at $r=r_i$, Eqn. (24) may be written as:

$$\frac{c_2}{2}\times\frac{n}{r_i^{\frac{2}{n}}}=\frac{\sigma_0}{P_2}\ell n.r_i-\frac{\rho\omega^2 r_i^{\,2}}{2}+c_3 \tag{27}$$

Subtracting Eqn. (27) from Eqn. (26), we get:

$$c_2\times\frac{n}{2}[\frac{1}{r_o^{\frac{2}{n}}}-\frac{1}{r_i^{\frac{2}{n}}}]=\frac{\sigma_0}{P_2}\ell n\frac{r_o}{r_i}+\frac{\rho\omega^2}{2}[r_i^{\,2}-r_o^{\,2}]$$

or

$$c_2=\frac{\frac{\sigma_0}{2}\ell n\frac{r_o}{r_i}+\frac{\rho\omega^2}{2}[r_i^{\,2}-r_o^{\,2}]}{\frac{n}{2}[\frac{1}{r_o^{\frac{2}{n}}}-\frac{1}{r_i^{\frac{2}{n}}}]} \tag{28}$$

Putting value of c_2 in equation (26) one may obtain c_3 given by:

$$c_3=\frac{n}{2\times r_o^{\frac{2}{n}}}\times\frac{\frac{\sigma_0}{2}\ell n\frac{r_o}{r_i}+\rho\omega^2(r_i^{\,2}-r_o^{\,2})}{\frac{n}{2}\times[\frac{1}{r_o^{\frac{2}{n}}}-\frac{1}{r_i^{\frac{2}{n}}}]}-\frac{\sigma_0}{P_2}\ell n.r_o+\frac{\rho\omega^2 r_o^{\,2}}{2} \tag{29}$$

Knowing c_2 and c_3 from Eqn. (28) and Eqn. (29) respectively, the radial stress, σ_r, may be obtained from Eqn. (24), which can be substituted in Eqn. (23) to obtain tangential stress, σ_θ, as given by:

$$\sigma_\theta=\frac{c_2}{r^{\frac{2}{n}}}+\frac{\sigma_0}{P_2}+\sigma_r \tag{30}$$

The effective stress is then calculated from Eqn. (11) and the tangential strain rate is calculated from Eqn. (22). Subsequently, the radial strain rate, $\dot{\varepsilon}_r=-\dot{\varepsilon}_\theta$, may also be known at different radial points of the cylinder.

CHAPTER 5

RESULTS AND DISCUSSIONS

Based on the analysis presented in chapter-4, the stress and strain rate distribution in the rotating cylinder have been obtained for various combination of particle size, *P,* particle content, *V,* and temperature of application, *T*. The values of the creep parameters have been taken from Table-1 as given in chapter-4. The *rpm* of the disc has been assumed to be 15,000. The value of stress exponent *n* in the Sherby's law given by Eqn. (5) is taken as 8, which correspond to lattice diffusion-controlled creep with a constant structure. Since the material of the disc is assumed to be isotropic, therefore, the values of the anisotropic constants (*F,G* and *H*) are set equal. The results obtained are discussed as below.

5.1 Effect of Material Parameters

5.1.1 Effect of Particle Size

Figs. (5.1-5.6) show the creep response of the composite cylinder for varying particle size of SiC reinforcement. It is noticed that in the region near the inner radius tangential stress increases rapidly and reaches a maximum value before decreasing near the outer radius as shown in Fig. (5.1). It is clearly evident that particle size does not have sizable effect on the tangential stress.

The radial stress as shown in Fig (5.2) also varies in a similar way with maximum value somewhere near the middle of the cylinder. Near the inner and the outer radii the radial stresses vanishes under the imposed boundary condition as given in Eqn. (25). The particle size, in this case too, has very little effect.

The axial stress as given by Eqn. (8) depends on the algebraic sum of tangential and radial stress. The variation of axial stress, as shown in Fig. (5.3), is similar to that observed for tangential stress in Fig. (5.1) but the values are higher than the tangential stress at the corresponding radial points. Similar to tangential and radial stresses, the axial stress is also marginally affected by particle size of the SiC reinforcement.

The distribution of strain rates as given by Eqs. (6) depends on the difference of effective

and the threshold stress, $(\bar{\sigma} - \sigma_0)$. Therefore, the effect of particle size on this stress difference has also been investigated as shown in Fig. (5.4). It is observed that the stress difference, $(\bar{\sigma} - \sigma_0)$ is significantly affected by varying particle size of the reinforcement. It has lowest value for the cylinder containing fine SiC_P of the size 1.7 μm and the highest values for the cylinder with coarse SiCp of size 45.9 μm over the entire cylinder radii. The order of variation of $(\bar{\sigma} - \sigma_0)$ with particle size is governed by magnitude of threshold stress, which decreases with increasing particle size as evident from Table-1.

The tangential strain rate, as shown in Fig. (5.5), decreases on moving from the inner towards the outer radius of the cylinder. The change in particle content of the reinforcement affects the tangential strain rate quite significantly as shown in Fig. (5.5). It is expected that smaller size particles will be larger in number for the same volume fraction and are able to restrain creep flow more effectively. The creep rate at any radius is reduced by almost three orders of magnitude when particle size decreases from 45.9 μm to 1.7 μm.

The variation of compressive radial strain rate with radial distance is shown in Fig (5.6). The strain rates decrease with radial distance with a minimum value at the outer radius. Like the tangential strain rate, radial strain rate is also reduced by almost three orders of magnitude over the entire disc radii when the particle size decreases from 45.9 μm to 1.7 μm. The cylinder containing SiCp of the size 1.7 μm shows the minimum creep rates due to lowest value of both, the stress difference $(\bar{\sigma} - \sigma_0)$ shown in Fig.(5.4) and the creep parameter *M* (Table-1) as compared to those in the cylinder containing coarse particles.

5.1.2 Effect of Particle Content

The effect of particle content on stress and strain rates in a rotating cylinder undergoing steady state creep are shown in Figs. (5.7)-(5.12). Near the inner radius of the disc, the tangential stress as shown in Fig. (5.7) is more for composite cylinder having lesser particle content but towards the outer radius the tangential stress is higher if cylinder containing more particle content. The tangential stress towards the outer radius of the cylinder decreases sharply in cylinder containing 10 *vol%* of SiC_P than that observed in a cylinder having 30 *vol %* of SiC_P. The effect of particle content on the radial stress, as

shown in Fig. (5.8), is similar to that observed for tangential stress in Fig. (5.7) near the inner radius of the cylinder. The radial stress decreases over the entire disc radii with increase in particle content from 10% to 30%. The maximum variation observed in the radial stress, when the particle content increases from 10% to 30%, is about 11%. The effect of particle content on axial stress, Fig. (5.9), is also similar to that observed for tangential stress in Fig. (5.7). The stress difference, $(\bar{\sigma} - \sigma_0)$, decreases significantly over the entire radius of the cylinder with increase particle content as shown in Fig. (5.10). As a consequence of significant reduction in stress difference, $(\bar{\sigma} - \sigma_0)$, Fig. (5.10), and creep parameter *M* (Table-1), with increase in SiC_P content, the tangential strain rate decreases significantly over the entire cylinder radius with increasing particle contents, as shown in Fig (5.11), when the particle content increases from 10% to 30% in a particle reinforced composite cylinder containing 1.7 μm SiC particles and operating at 623 *K*. The tangential strain rate decreases by about six orders of magnitude when the particle content increases from 10% to 30%. The variation of radial strain rate with radial distance for varying particle content is shown in Fig (5.12). The effect of increasing particle content from 10% to 30% on radial strain rate is similar to that observed previously for tangential strain rate in Fig. (5.11). Thus, it appears that with increasing particle content the inter-particle spacing in composite decreases which is responsible for reduction in strain rates.

5.2 Effect of Operating Temperature

Temperature is one of the key factors influencing creep flow of any material. In this section, the effect of the variation of temperature on stress distributions and creep deformations is reported for a rotating cylinder made of aluminum base particle reinforced composite containing 20 *vol %* SiC particles of size 1.7 μm.

Fig. (5.13) shows the distribution of tangential stress with radial distance in a rotating cylinder at three temperature level *i.e.* 623 K, 673 K and 723 K. It is observed that tangential stress varies a little when the temperature is increased from 623 K to 723 K. Similarly, the temperature also very little effect on radial and axial stress distributions, as shown in Fig. (5.14) and Fig. (5.15) respectively. However, the stress difference $(\bar{\sigma} - \sigma_0)$

shows sizable variation with varying temperatures as evident from Fig. (5.16). It reduces by about 4.6% over the entire cylinder radii when the temperature increases from 623 *K* to 723 *K*. It may be attributed to a little increase in threshold stress with increasing temperature, Table-1.

In spite of very small change in tangential and radial stress, and stress difference, $(\overline{\sigma} - \sigma_0)$, with temperature, the tangential strain rates at different temperature are quite different as shown in Fig (5.17). The tangential strain rate increases by about three orders of magnitude as the operating temperature increases from 623 *K* to 723 *K*. The effect of temperature on radial strain as shown in Fig. (5.18), is also similar to that observed for tangential strain rate in Fig. (5.17). The significant increase in strain rates with increase in temperature may be attributed to increase in creep parameter *M* with increasing temperature although, the stress difference, $(\overline{\sigma} - \sigma_0)$, as shown in Fig. (5.16) decreases with increasing temperature.

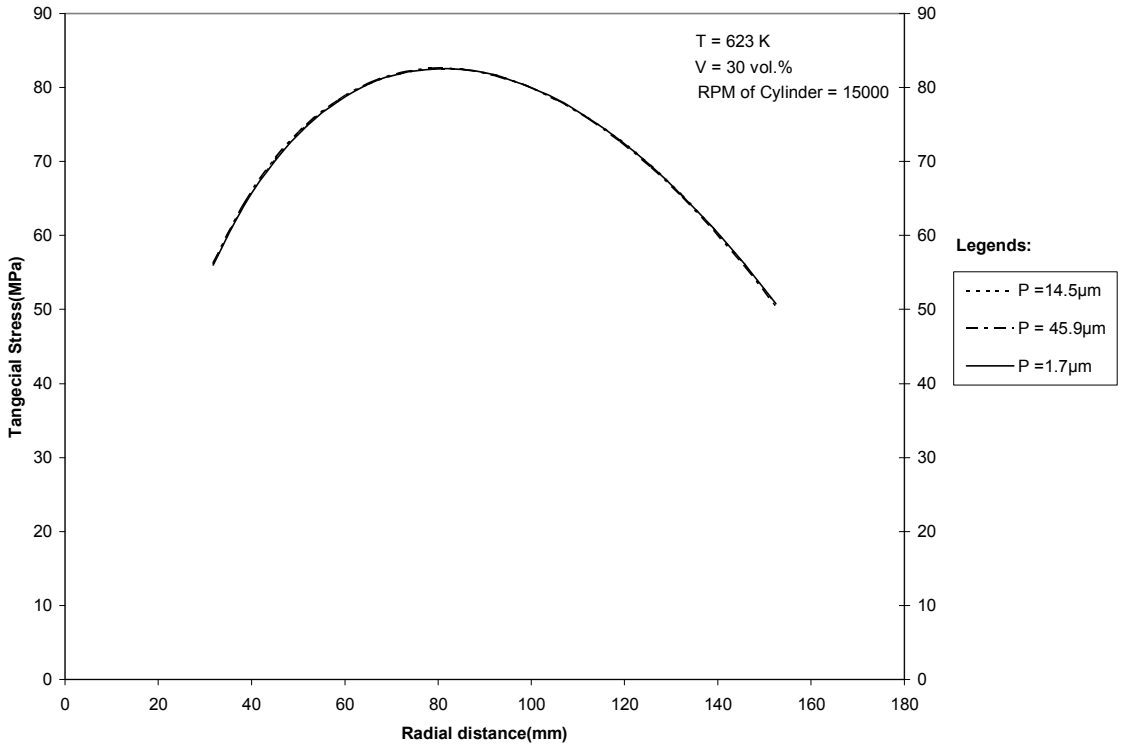

Fig.5.1 Effect of Particle Size on Tangential Stress.

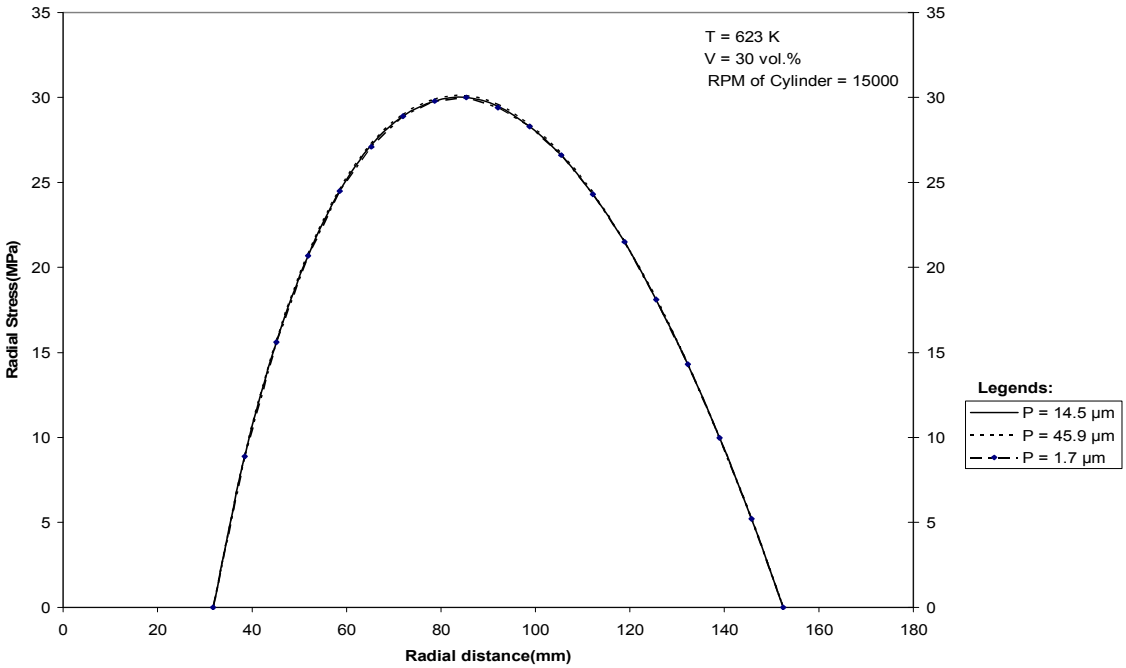

Fig.5.2 Effect of Particle Size on Radial Stress.

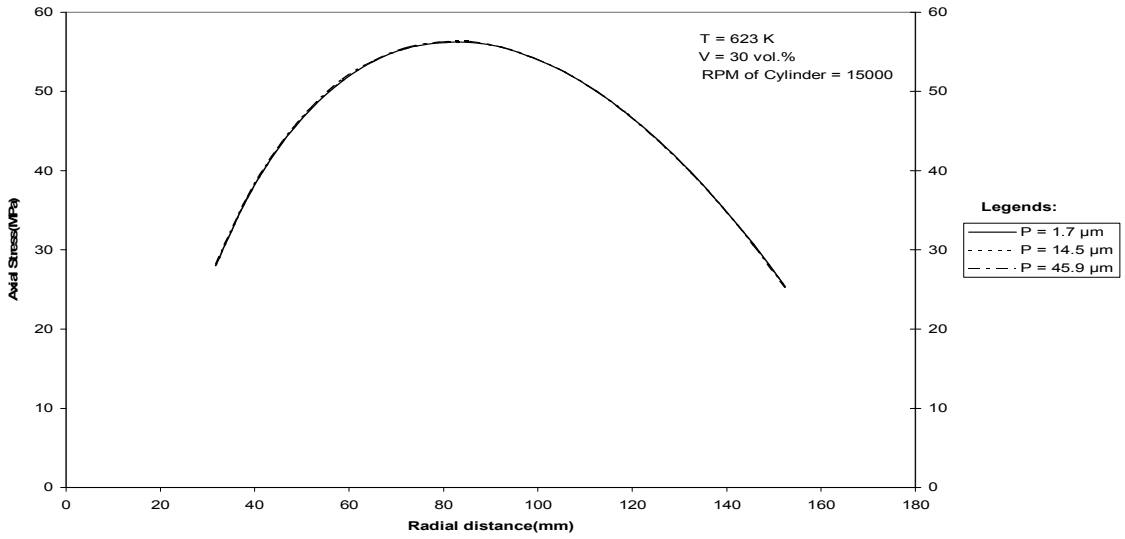

Fig.5.3 Effect of Particle Size on Axial Stress.

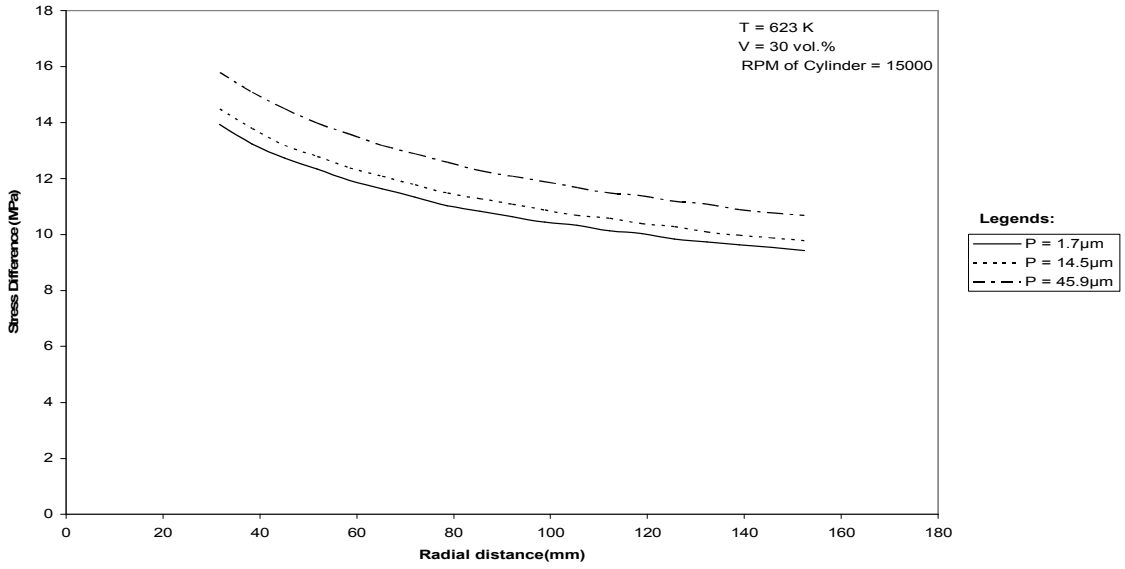

Fig.5.4 Effect of Particle Size on Stress Difference ($\overline{\sigma} - \sigma_0$).

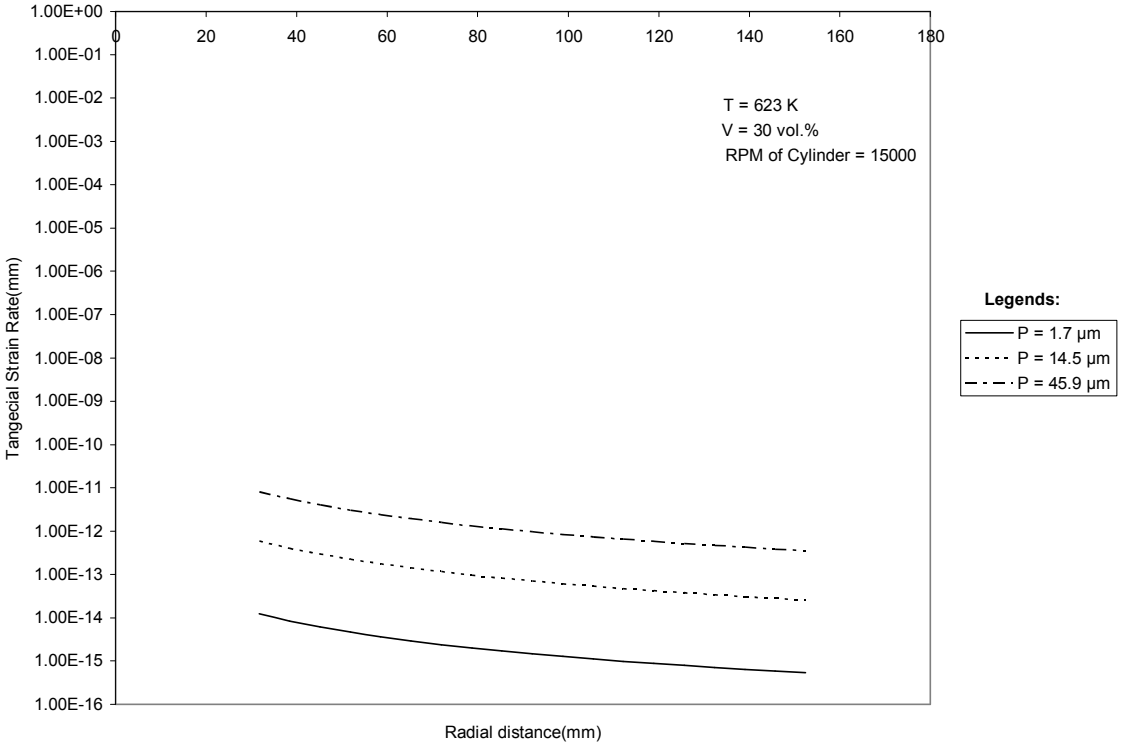

Fig.5.5 Effect of Particle Size on Tangential Strain Rate.

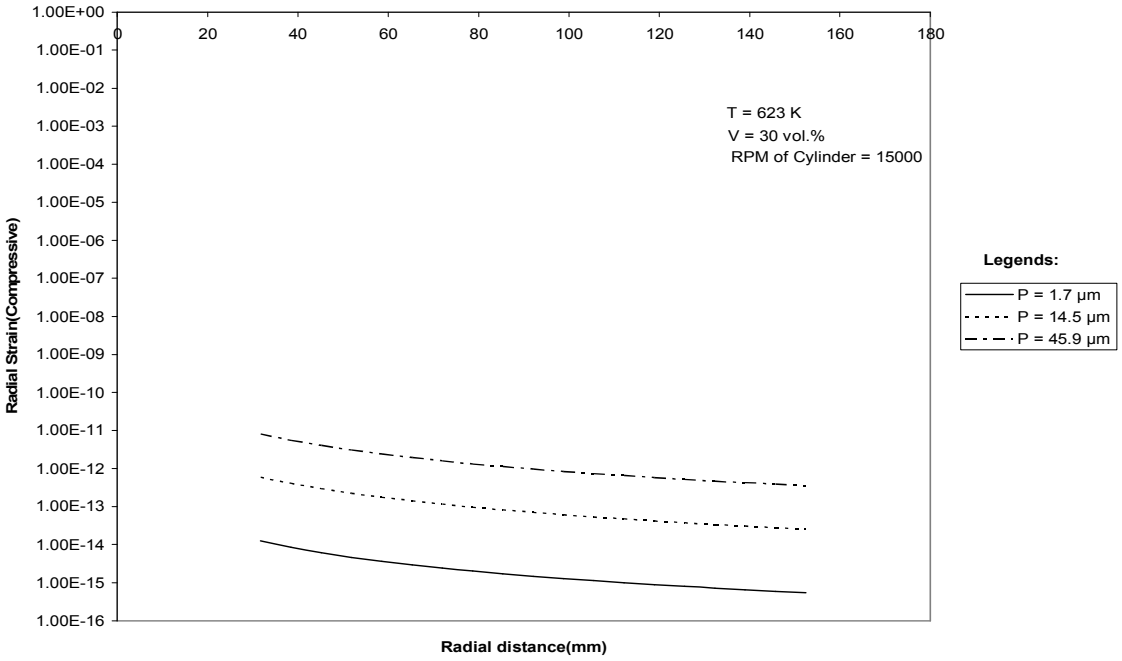

Fig.5.6 Effect of Particle size on Radial Strain Rate.

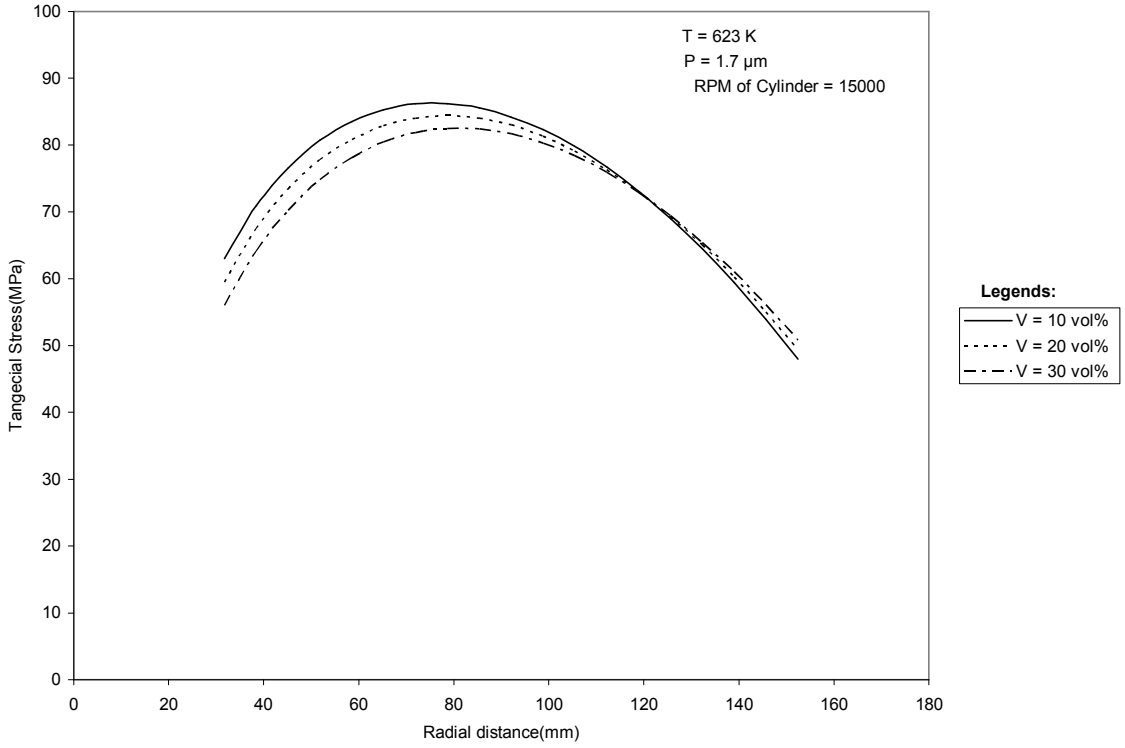

Fig.5.7 Effect of Particle Volume on Tangential Stress.

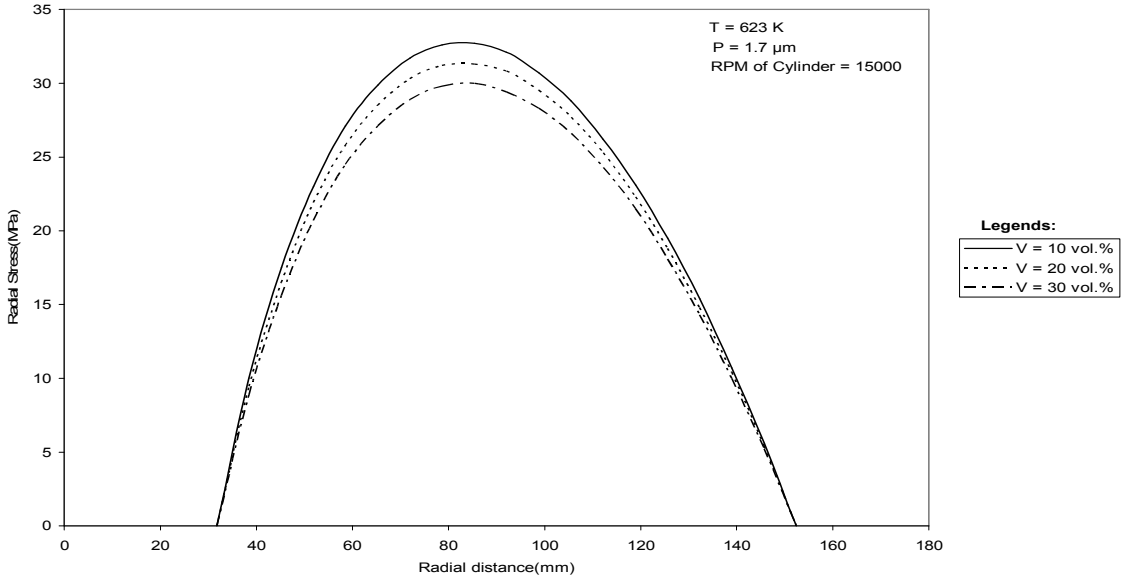

Fig.5.8 Effect of Particle Volume on Radial Stress.

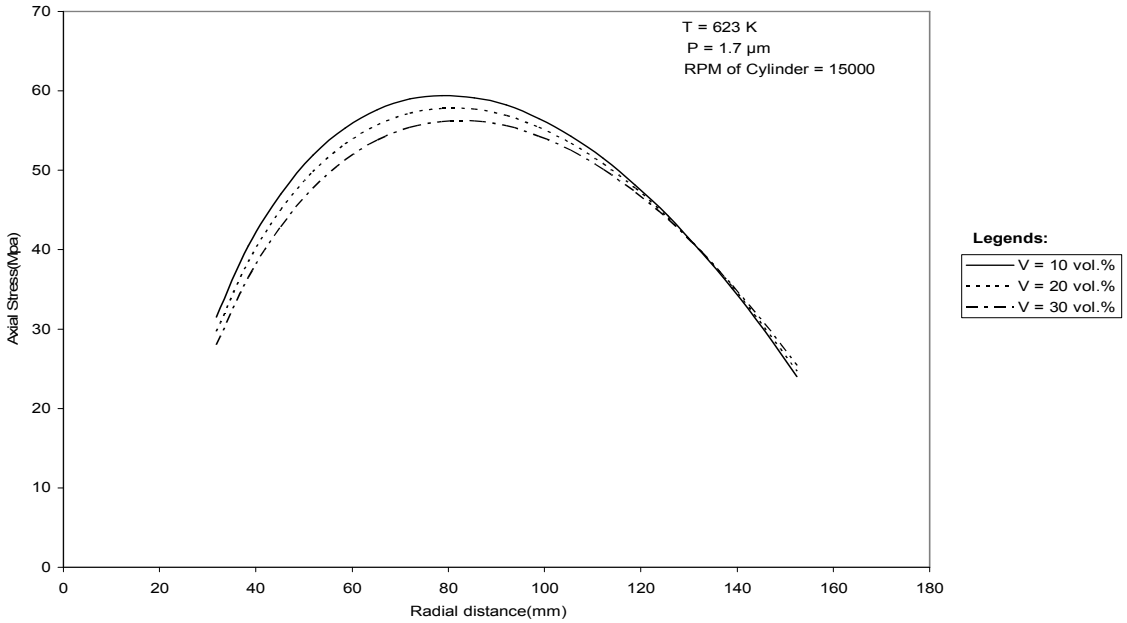

Fig.5.9 Effect of Particle Volume on Axial Stress.

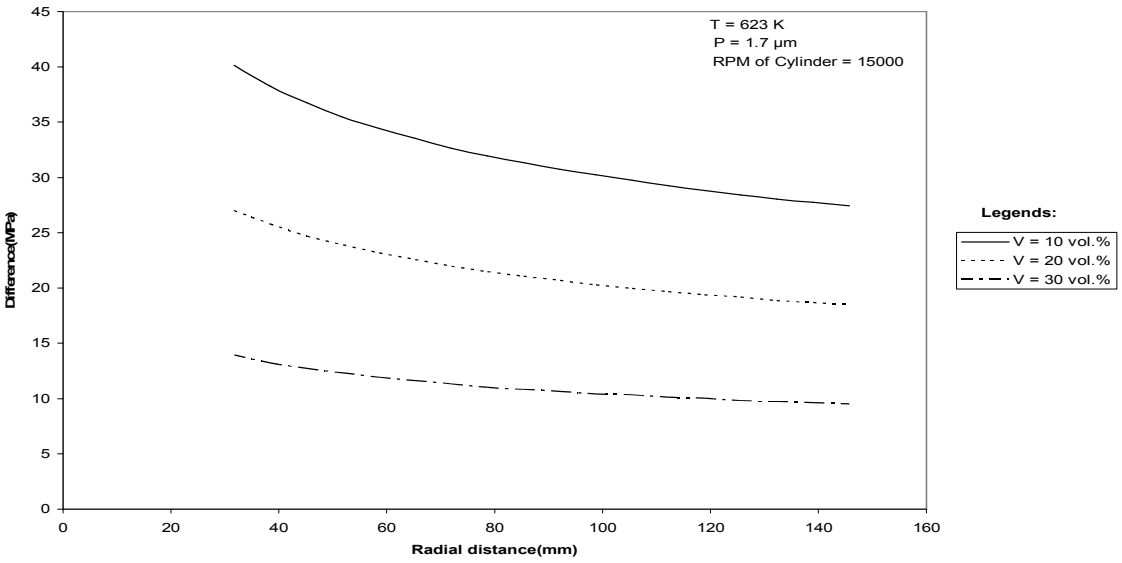

Fig.5.10 Effect of Particle Volume on Stress Difference ($\overline{\sigma} - \sigma_0$).

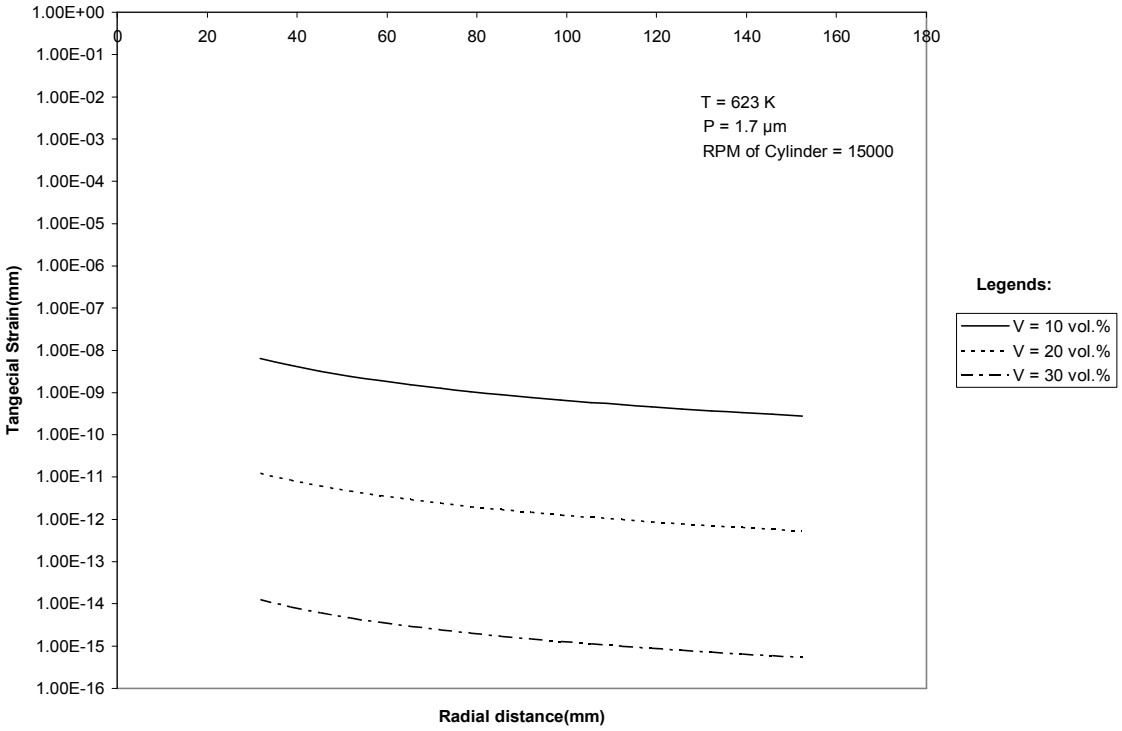

Fig.5.11 Effect of Particle Volume on Tangential Strain Rate.

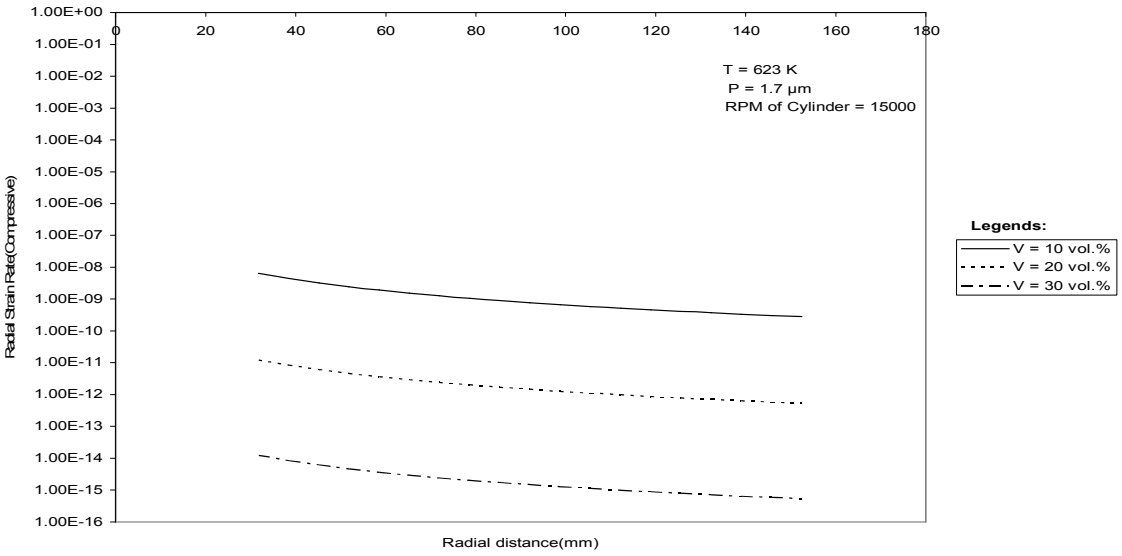

Fig.5.12 Effect of Particle Volume on Radial Strain Rate.

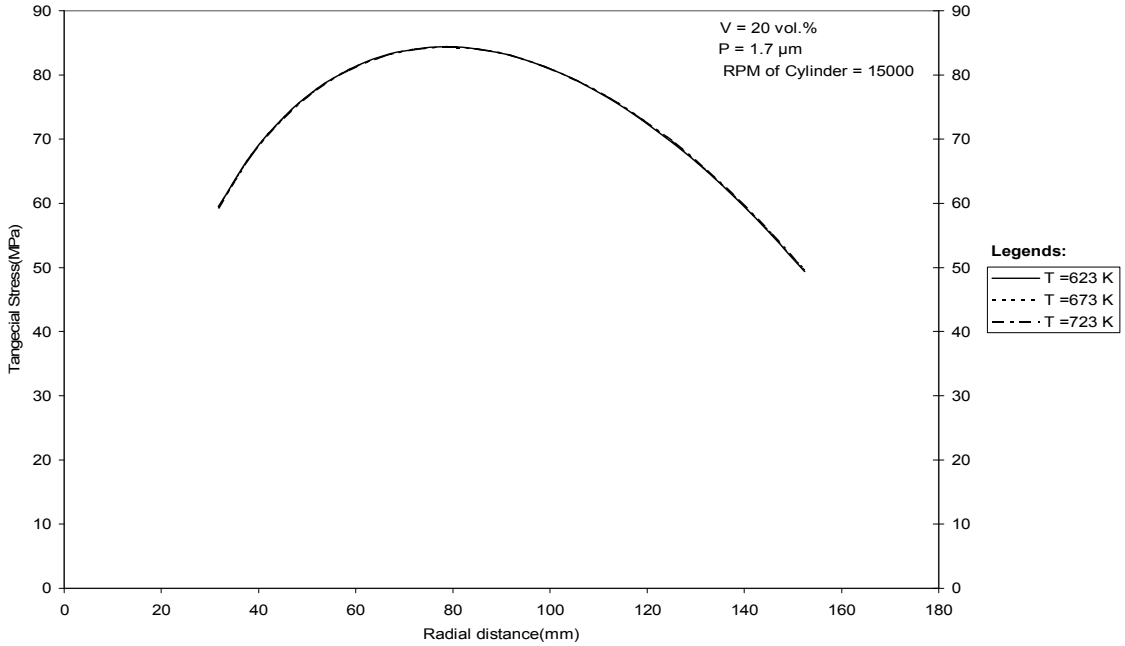

Fig.5.13 Effect of Temperature Variation on Tangential Stress.

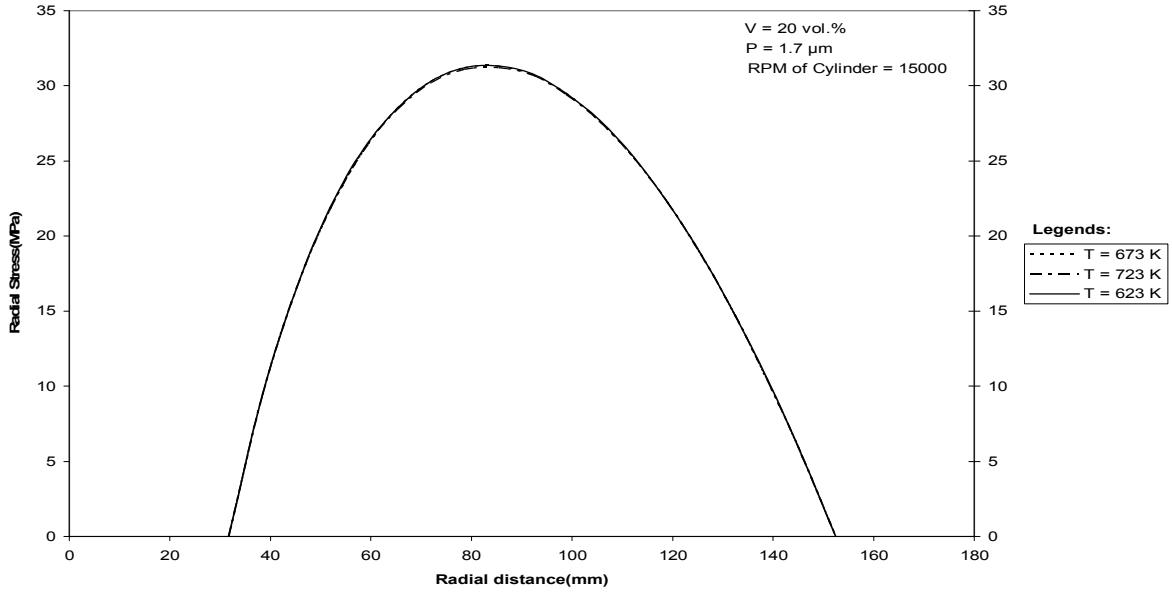

Fig.5.14 Effect of Temperature variation on Radial Stress.

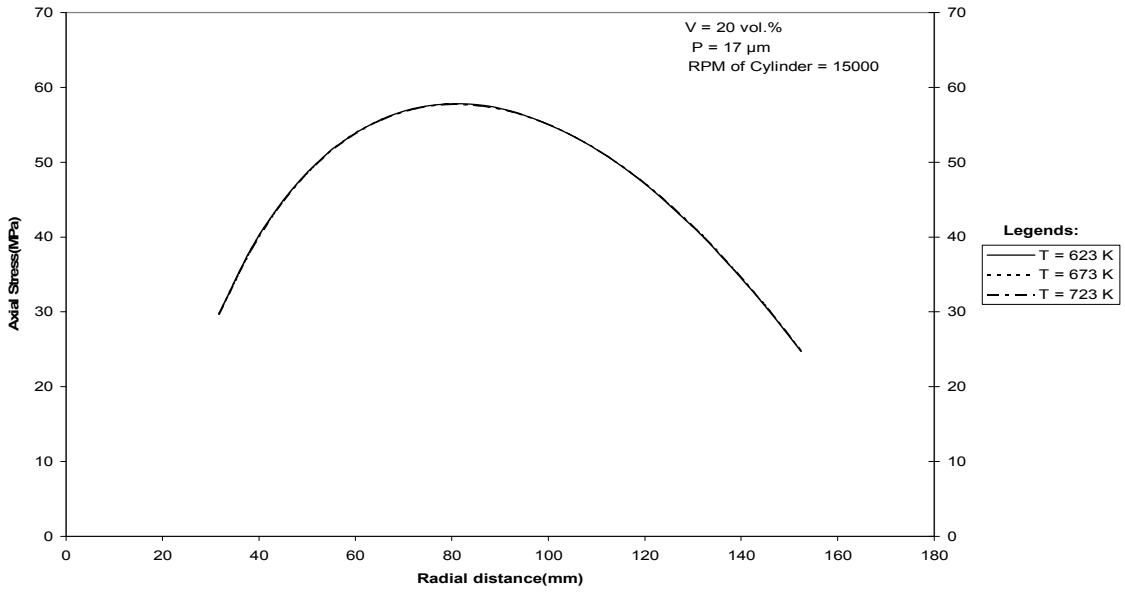

Fig.5.15 Effect of Temperature Variation on Axial Stress.

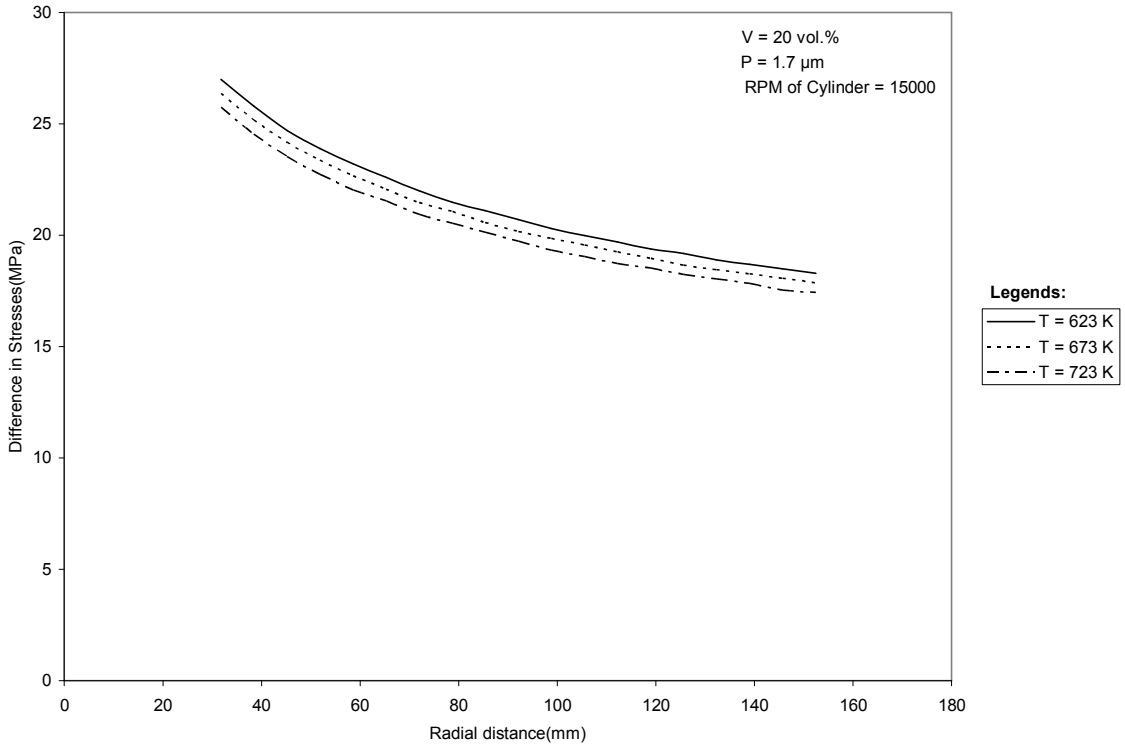

Fig.5.16 Effect of Temperature Variation on Stress Difference ($\overline{\sigma} - \sigma_0$).

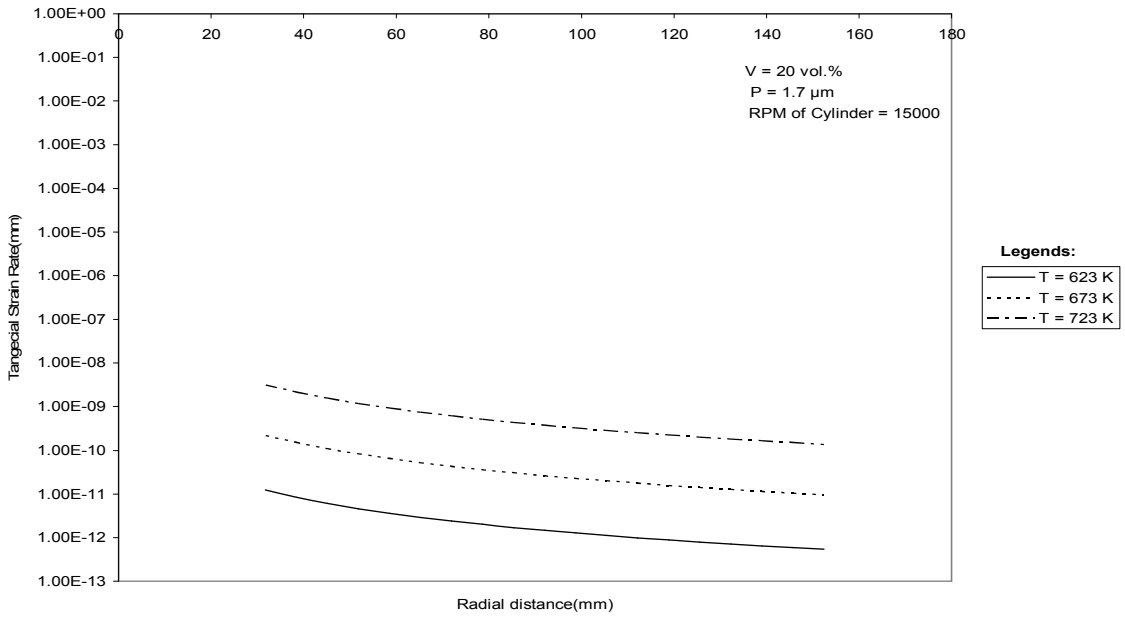

Fig.5.17 Effect of Temperature Variation on Tangential Strain Rate.

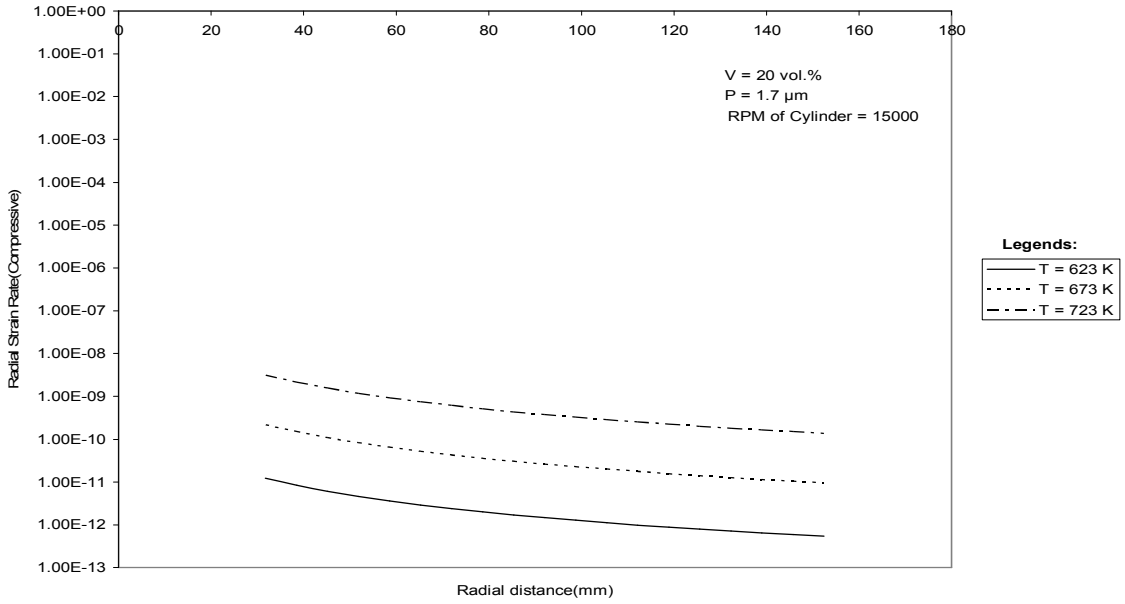

Fig.5.18 Effect of Temperature Variation on Radial Strain Rate.

CHAPTER 6

CONCLUSIONS

Based on results and discussions presented in chapter-6, the following conclusions may be drawn:

a) The radial, tangential and axial stresses increases, as we move from inner towards outer radius of cylinder, reaches maximum before decreasing near the outer radius.

b) The stress distributions in the cylinder do not vary significantly for various combinations of particle size and operating temperature. The increase in particle content shows sizable variation on stress distributions in cylinder.

c) The stress difference $(\sigma_e - \sigma_0)$, decreases significantly over the entire cylinder radii with decreasing particle size, increasing particle content and increasing temperature.

d) The tangential as well as radial strain rate decreases on moving from inner towards outer radius of the cylinder.

e) The tangential as well as radial strain rates in a rotating isotropic Al-SiC_p cylinder decrease significantly with decreasing SiC_p size, with increasing SiC_p content and with decreasing operating temperature.

Scope for Future Work

The study carried out in this thesis may be further extended in the following directions:

- Creep behavior of rotating cylinder made of other composite materials may also be investigated.
- The effect of anisotropy may also be investigated on the creep performance of rotating composite cylinder.
- The analysis may be extended for creep behavior of rotating cylinder subjected to (i) internal pressure and (ii) internal as well as external pressure.
- The analysis carried out in this work may be repeated for creep laws based on stress exponent n=3 and n=5, and its effect on creep stresses and strain rates in a rotating cylinder may be investigated.
- The analysis may be extended for composite cylinder made of Functionally Graded Materials (FGMs).

REFERENCES

[1] Autar K. Kaw, "Mechanics of Composites Materials", CRC Press Boca Raton, New York, pp.2-18, 1997.

[2] V. K. Lindroos and M. J. Talvitie, "Recent Advances in Metal Matrix Composites", *Helsinki University of technology, Laboratory of Physical Metallurgy and Materials Science*,Finland,pp.274-279,1995.

[3] W. H. Hunt, Jr. "Metal Matrix Composites", *Aluminium Consultants Group, Inc., Murrysville*, PA, USA,pp.2-7,2000.

[4] George E. Deiter, "Mechanical Metallurgy", McGraw-Hill Book Company, Maryland, 1928.

[5] S. B. Singh and S. Ray, "Newly Proposed Yield Criteria for Residual Stress and Steady State Creep in an Anisotropic Rotating Composite Disc", *J. Mater Proc. Tech,* vol .143-144,pp.623-628,2003.

[6] S. C. Tjong and Z. Y. Ma, "Microstructural and mechanical Characteristics of in-situ Metal Matrix Composites", *Mater. Sci. Engg.*, A-29 pp. 49-113, 1999.

[7] E.A.Davis and F.M.Connelly, "Stress Distribution and Plastic Deformation in Rotating Cylinders of Strain-Hardening Material", ASME *Journal of Applied Mechanics*, Vol. 26, No. 1, Mar. 1959, pp. 25-30.

[8] F.P.J.Rimrott, "Creep of Thick-Walled Tubes Under Internal Pressure Considering Large Strains",*Journal of Applied Mechanics*, June 1959.

[9] I.N.Danilova, "On Calculation of the Stresses State in a Rotor during Transient Creep", *IZV, ANSSAR.OTN, Mechanics and Engineering*, No. 5, 1959.

[10] Y.N.Rabotnov, "Possibilities of Describing Transient Creep in Application to Creep in Rotors", *IZV, ANSSAR.OTN,* No. 5, 1959.

[11] Y.N.Rabotnov, "Creep of Rotating Cylinder and Tube" *Creep Problems in Structural Members*, North-Holland, Amsterdam, 1969, pp. 679-684.

[12] Dipti Dev, "Note on Creep of a Cylinder Rotating about Its axis", *Int. .r of Math and Mech.*, Vol 3, pp 104-107,1961.

[13] N.S.Bhatnagar and V.K.Arya, "Large Strain Creep Analysis of Thick-Walled Cylinder",*International Journal of Non-Linear Mechanics*, Vol.9, No.2, pp 127-140,1974.

[14] V.K.Arya, K.K.Debnath and N.S.Bhatnagar, "The Spherical Vessel with Creep Properties Considering Large Strains", *Int. J. Press. Vess. Piping*, Vol 15, Issue 3, pp 185-193, 1980.

[15] N.S.Bhatnagar, V.K.Arya and K.K.Debnath, "Creep Analysis of Orthotropic Rotating Cylinder", *J. of Press. Vess. Tech.,* Vol. 102, pp. 371-377, Nov. 1980.

[16] S.K.Gupta and R.L.Dharmani, "Creep Tranisition in Rotating Cylinder",*J.Math.Phy* Vol 15,No.6,1981.

[17] Suresh Hulsurkar, "Transition Theory of Creep of Composite Cylinder Under Uniform Internal Pressure",*Journal Math Physics Science*, Vol.15,No.4, 1981.

[18] V.K.Arya, K.K.Debnath and N.S.Bhatnagar, "Creep Analysis of Orthotropic Circular Cylinderical Shells", *Int. J. Press. Vess. Piping*, Vol 11, pp 167, 1983.

[19] F.P.J.Rimrott and J.R.Luke, "Large strain Creep of Rotating Cylinder",*Z.agnew Math.Mech.*,Vol 41,pp 485,1984.

[20] N. S. Bhatnagar, P. S. Kulkarni and V. K. Arya, "Steady State Creep of Orthotropic Rotating Discs of Variable Thickness", *Nuclear Engineering and Design,* vol.91, pp. 121-141, 1986.

[21] N.S.Bhatnagar, P.S.Kulkarni and V.K.Arya, "Creep Analysis of Orthotropic Rotating Cylinder Considering Finite Strains", *Int. J. Non-Liner Mechanics*, Vol.21, No.1, pp 61-71, 1986.

[22] S.K.Gupta and Sonia Pathak, "Thermo Creep Transition in Walled Circular Cylinder Under Internal Pressure", *Indian J.Pure Applied Math*, Vol 32 (2), pp 237-253, 2001.

[23] Jerome T. Tzeng, Army Research Lab Aberdeen Proving Ground MD.2003.

[24] V.K.Gupta, S.B.Singh, H.N.Chandrawat and S. Ray, "Steady State Creep and Material Parameters in a Rotating Disc of Al-SiC_P Composite", *European Journal of Mechanics A/Solids,* Vol. 23, pp. 335-344, 2004.

[25] A.B.Pandey, R.S.Mishra and Y.R.Mahajan, “Steady State Creep Behaviour of Silicon Carbide Particulate Reinforced Aluminium Composites,” Acta Metall. Mater., Vol. 40(8), pp. 2045-2052., 1992.

APPENDIX

```
#include<iostream.h>
#include <stdio.h>
#include <conio.h>
#include <stdlib.h>
#include <math.h>
const int DIV=18;
float Ri=31.75;
float Ro=152.4;
float dx=(Ro-Ri)/DIV;
void main ()
{
      clrscr();
      int l=DIV;
      FILE *fout;
      fout=fopen("sachan.dat","w");
      if(!fout)
      {
       printf("CAN'T OPEN SHERBY1.DAT FOR INPUT !!! \n");
       exit(0);
      }
      printf("\n" "ENTER CHOICE 1 IF NON-FGM ISOTROPIC\n"
               " ENTER CHOICE 2 IF NON-FGM ANISOTROPIC (LONGITUDINAL IS
TANGENTIAL)\n"
               " ENTER CHOICE 3 IF NON-FGM ANISOTROPIC (LONGITUDINAL IS
Radial)\n"
               " ENTER CHOICE 4 IF NON-FGM ANISOTROPIC (LONGITUDINAL IS
Z-Direction)\n");
      int CHOICE;
      printf ("ENTER CHOICE=");
      scanf ("%d",& CHOICE);
      printf("\n  F\t\t G\t    H\t\tV\t"
               "sgl\tsgt\t m\t sigma0\t \n");
      fprintf(fout,"\n  F\t\t G\t    H\t\tV\t"
               "sgl\tsgt\t m\t c\t \n");
      float
stress_r[DIV+1],Rad[DIV+1],stress_t[DIV+1],stress_z[DIV+1],strain_r[DIV
+1],strain_t[DIV+1],strain_z[DIV+1],sigma0[DIV+1];
      float T=623.0, P=1.7, V=30.0;
      float rho=(2680*V+3200*(100-V))/100;
      int i;
      float m[DIV+1],f[DIV+1],g[DIV+1],h[DIV+1];
      float omega=2*3.1415927*15000/60;
for (i=0;i<=l;i++)
{
// for Al-SiCp (Isotropic disc) to study effect of P,T and V
      m[i]=exp(-35.38)*pow(P,0.2077)*pow(T,4.98)*pow(V,-0.622);
      sigma0[i]=(-0.03507*P+0.01057*T+1.00536*V-2.11916);
/*
// for 6061Al-SiCp (Isotropic and Anisotropic
      m[i]=exp(-35.38)*pow(P,0.2077)*pow(T,4.98)*pow(V,-0.622)
                              -0.0395+1.2994*pow(10,-4)*T-
1.0003*pow(10,-7)*T*T;
```

```
      sigma0[i]=(-0.03507*P+0.01057*T+1.00536*V-2.11916
                              -116.441+0.8002*T-9.644*pow(10,-4)*T*T);
*/
      if (CHOICE==2)
      {
      //tangential is longitudinal
      f[i]=h[i]=0.5/pow(2.758*(100-V)-1.0920*V,2);//rule of mixture
      g[i]=pow((100-V)/27580+V/3932.032,2)-f[i];
      }
      else if (CHOICE==3)
      {
      //radial is longitudinal
      g[i]=h[i]=0.5/pow(2.758*(100-V)-1.092*V,2);//rule of mixture
      f[i]=pow((100-V)/27580+V/3932.032,2)-g[i];
      }
      else if (CHOICE==4)
      {
      //Z-is longitudinal
      g[i]=f[i]=0.5/pow(2.758*(100-V)-1.092*V,2);//rule of mixtr
      h[i]=pow((100-V)/27580+V/3932.032,2)-g[i];
      }
      else if (CHOICE==1)
      {
      // for isotropic Von Mises
//    h[i]=g[i]=f[i]=1.0;
      h[i]=g[i]=f[i]=0.5/pow(2.758*(100-V)-1.092*V,2);//rule of mixtr
      }
      printf("%10.2e %10.2e %10.2e %8.2f %8.2f %8.2f %8.4f %8.4f\n",
    f[i],g[i],h[i],V,(2.758*(100-V)-1.092*V),1/((100-
V)/27580+V/3932.032),m[i],sigma0[i]);
fprintf(fout,"%10.2e %10.2e %10.2e %8.2f %8.2f %8.2f %8.4f %8.4f\n",
f[i],g[i],h[i],V,(2.758*(100-V)-1.092*V),1/((100-
V)/27580+V/3932.032),m[i],sigma0[i]);
}
       getch();
       printf("\nRadius   stress_r   stress_t   stress_z    str_eff
strain_t  strain_r\n");
      fprintf(fout,"    Radius   stress_r   stress_t   stress_z
strain_t  strain_r    strain_z\n");
   for (i=0;i<=l;i++)
      {
               float R=Ri+i*dx;
               float
P2=pow((f[i]*g[i]+g[i]*h[i]+h[i]*f[i])/((f[i]+g[i])*(g[i]+h[i])),0.5);
               float K=0.5*pow(m[i],8)*pow(P2,4.5)*(g[i]+h[i]);
               float t=0.25;
               float dummy1=pow(Ro,t);
               float dummy2=pow(Ri,t);
               float dummy3=pow(R,t);
               float
NMR_C2=sigma0[i]*(log(Ro/Ri))/P2+rho*omega*omega*pow(10,-12)*(Ri*Ri-
Ro*Ro)/2;
               float DNR_C2=4.0*((1/dummy1)-(1/dummy2));
               float C2=NMR_C2/DNR_C2;
               float C3=8*C2/(2*dummy1)-
sigma0[i]*log(Ro)/P2+rho*omega*omega*pow(10,-12)*Ro*Ro/2;
               if(i==0||i==l)stress_r[i]=0;
```

```
                else stress_r[i]=-
((C2)/2)*(8/dummy3)+((sigma0[i]/P2)*log(R))-((rho*omega*omega*pow(10,-
12)*R*R)/2)+C3;
                stress_t[i]=(C2/dummy3)+stress_r[i]+sigma0[i]/P2;

stress_z[i]=(g[i]*stress_r[i]+f[i]*stress_t[i])/(f[i]+g[i]);
                float sigma_eff[20];
                sigma_eff[i]=P2*(stress_t[i]-
stress_r[i]);//printf("sigma%f\n",sigma_eff[i]);
                float C1=pow(C2,8)*K;
                if (sigma_eff[i]>sigma0[i])
                {
                      strain_t[i]=C1/(R*R);
                      strain_r[i]=- strain_t[i];
                      strain_z[i]=0;
                }
                else
                {     strain_t[i]=0;
                      strain_r[i]=0;
                      strain_z[i]=0;
                }
                printf("%6.2f%10.2e %10.2e %10.2e %10.2e %10.2e
%10.2e\n",R,stress_r[i],stress_t[i],stress_z[i],sigma_eff[i],strain_t[i
],strain_r[i]);
                fprintf(fout,"%d->%f%10.2e %10.2e %10.2e %10.2e %10.2e
%10.2e\n",i,Rad[i],stress_r[i],stress_t[i],stress_z[i],strain_t[i],stra
in_r[i],strain_z[i]);
           }
            getch();
}
```